

**DOT/FAA/AR-09/50**

Air Traffic Organization  
NextGen & Operations Planning  
Office of Research and  
Technology Development  
Washington, DC 20591

# **The Effects of Operating Jet Fuels Below the Specification Freeze Point Temperature Limit**

January 2010

Final Report

This document is available to the U.S. public  
through the National Technical Information  
Service (NTIS), Springfield, Virginia 22161.



U.S. Department of Transportation  
**Federal Aviation Administration**

## **NOTICE**

This document is disseminated under the sponsorship of the U.S. Department of Transportation in the interest of information exchange. The United States Government assumes no liability for the contents or use thereof. The United States Government does not endorse products or manufacturers. Trade or manufacturer's names appear herein solely because they are considered essential to the objective of this report. This document does not constitute FAA certification policy. Consult your local FAA aircraft certification office as to its use.

This report is available at the Federal Aviation Administration William J. Hughes Technical Center's Full-Text Technical Reports page: [actlibrary.tc.faa.gov](http://actlibrary.tc.faa.gov) in Adobe Acrobat portable document format (PDF).

1. Report No. DOT/FAA/AR-09/50		2. Government Accession No.		3. Recipient's Catalog No.	
4. Title and Subtitle THE EFFECTS OF OPERATING JET FUELS BELOW THE SPECIFICATION FREEZE POINT TEMPERATURE LIMIT				5. Report Date January 2010	
				6. Performing Organization Code	
7. Author(s) Steven Zabarnick and Jamie Ervin				8. Performing Organization Report No.	
9. Performing Organization Name and Address University of Dayton Research Institute 300 College Park Dayton, OH 45469-0116				10. Work Unit No. (TRAIS)	
				11. Contract or Grant No. DTFA03-01-C-00038	
12. Sponsoring Agency Name and Address U.S. Department of Transportation Federal Aviation Administration Air Traffic Organization NextGen & Operations Planning Office of Research and Technology Development Washington, DC 20591				13. Type of Report and Period Covered Final Report November 2001 to February 2004	
				14. Sponsoring Agency Code ANE-110	
15. Supplementary Notes The Federal Aviation Administration Airport and Aircraft Safety R&D Division technical monitor was Stewart Byrnes.					
16. Abstract <p>In the United States, commercial jet aircraft operations are currently limited to measured wing tank fuel temperatures that are greater than 3°C above the fuel specification freeze point. In recent years, long-duration polar routes have been open, which result in fuel being subjected to lower temperatures for longer periods. When the measured in-tank fuel temperature approaches these low-temperature limits, pilots are forced to modify flight path, altitude, and/or airspeed to raise these temperatures. As many fuel samples have freeze points that are significantly below the fuel specification, airlines would like to change the low-temperature operational limit to reflect the measured freeze point of the particular fuel sample in the aircraft fuel tank, rather than the specification freeze point. This could minimize unnecessary flight path, altitude, and/or airspeed alterations with significant cost savings.</p> <p>This report summarizes the study of the effect of low temperatures on jet fuel properties and fuel system operation. An aircraft wing tank simulator was designed and constructed that can be subjected to low temperatures inside an environmental chamber. The simulator employs actual Boeing 747 fuel hardware, such as a boost pump and flapper valves. The fuel flow rates, temperature profiles, pressures, and pump power are measured as a function of temperature. A series of laboratory studies were performed to better characterize fuel properties at these low temperatures, such as scanning Brookfield viscometry measurements; normal alkane chromatographic analyses; and freeze, cloud, and pour point measurements. The increased fuel viscosity at these low temperatures results in significant reductions in flowability and pumpability. Fuels with low freeze points display increased viscosity near their freeze point relative to higher-temperature freeze point fuels. The implications of these findings are likely fuel system dependent. Computational fluid dynamics studies of the wing tank simulator allow prediction of fuel temperatures in real fuel systems. The computational results show that the presence or absence of ullage space greatly affects fuel tank vertical temperature profiles. The results show the importance of the location of fuel temperature sensors in obtaining accurate measurements of the lowest fuel temperatures in the tank. In addition, the implications of adopting the Jet A-1 standard and the use of fuel system heaters on low-temperature fuel system operation are discussed.</p>					
17. Key Words Low-temperature fuel system operation, Viscosity, Flowability, Freeze point			18. Distribution Statement This document is available to the U.S. public through the National Technical Information Service (NTIS), Springfield, Virginia 22161		
19. Security Classif. (of this report) Unclassified		20. Security Classif. (of this page) Unclassified		21. No. of Pages 70	22. Price

## ACKNOWLEDGEMENTS

This work was supported by the Federal Aviation Administration, Airport and Aircraft Safety Research and Development Division. The authors would like to acknowledge Ms. Cindy Obringer and Mr. Bill Harrison of the U.S. Air Force Research Laboratory (AFRL) Fuels Branch and National Aerospace Fuels Research Complex for allowing use of their low-temperature fuels facilities for this study. In addition, the authors would like to thank Mr. Dino Scanderbeg of Hydro-Aire for the loan of the fuel boost pump, Mr. Kevin Longwell of Boeing for the wing tank photographs and help in understanding the Boeing 747 wing tank and fuel system, and Mr. Francis Davidson and Dr. Gordon Chiu of Phase Technology for the Jet A freeze point data. The authors would like to thank Mr. Mark Laber of the University of Dayton Research Institute (UDRI) for performing the wing tank simulator runs and Ms. Rajee Assudani of UDRI for performing the computational fluid dynamics calculations. The authors would also like to thank Ms. Linda Shafer and Mr. Marlin Vangsness of UDRI for the viscosity measurements and Mr. Dave Goller of AFRL for the freeze, cloud, and pour point measurements.

## TABLE OF CONTENTS

	Page
EXECUTIVE SUMMARY	xiii
1. INTRODUCTION	1
2. LABORATORY STUDIES	4
2.1 Scanning Brookfield Viscometry	4
2.2 Normal Alkane Measurements	7
2.3 Studies of the Intermingling of Fuels	9
3. WING TANK SIMULATOR STUDIES	13
4. COMPUTATIONAL FLUID DYNAMIC MODELING OF FUEL TEMPERATURES IN AIRCRAFT WING TANK SIMULATORS	21
4.1 Simulation Methodology	21
4.2 Simulations of Boeing and Lockheed Static-Cooling Experiments	25
4.2.1 Lockheed Tank Simulations	25
4.2.2 Boeing Tank Simulations	28
4.3 Simulations of Fuel Cooling Within the Wing Tank Simulator	29
4.3.1 Two-Dimensional Simulations	29
4.3.2 Three-Dimensional Simulations	41
4.4 Modeling Summary	44
5. OTHER ISSUES	45
5.1 Implications of Adopting the Jet A-1 Standard	45
5.2 Fuel System Heating	46
6. CONCLUSIONS	46
7. RECOMMENDATIONS	47
8. REFERENCES	47

## APPENDICES

A—Figures and Drawings of the Boeing 747 Wing Tank and Fuel System

B—Photographs of the Wing Tank Simulator

C—Boost Pump Information

D—Wing Tank Simulator Runs Performed

## LIST OF FIGURES

Figure		Page
1	Frequency of Occurrence of Fuel Freeze Points for Jet A Fuels Measured at North American Airports	1
2	Scanning Electron Micrograph of Normal Alkane Crystals	2
3	Chromatogram of a Jet A Fuel Showing the Normal Alkane Distribution	2
4	Lockheed Data Showing Vertical Temperature Profiles at Various Locations in a Wing Tank Simulator	3
5	Measured Viscosity vs Temperature for Nine Jet A Fuel Samples	5
6	Viscosity vs Temperature for the Liquid-Phase Region for Nine Jet A Fuel Samples	6
7	Weight Percent of the Normal Alkanes for the 12 Fuels Studied	8
8	Hypothetical Ideal Mixture Freeze Point Behavior for the Mixing of Two Fuels	10
9	Hypothetical Mixture of Two Fuels With the Mixture Producing a Fuel With a Higher Freeze Point Than the Original Fuels	10
10	Freeze Points for Mixtures of Two Fuels, 3686 and 3633, Showing Near Linear Behavior	11
11	Measured Freeze Point vs Percentage of Fuel 3775 in Mixtures of Fuel 3775 With Fuel 3686 Showing Nonlinear Behavior	12
12	Measured Freeze Point vs Percentage of Fuel 3633 in Mixtures of Fuel 3775 With Fuel 3633	13
13	A Boeing 747 Showing Location of Fuel Tanks	14
14	The Wing Tank Simulator	15
15	Wing Tank Simulator Showing Boost Pump, Turbine Flowmeter, Valve, and Film Heaters	16
16	Temperature Profiles in the Wing Tank Simulator (a) Temperatures at Three Vertical Locations During Cooldown and (b) Vertical Temperature Profiles at Three Different Times During Cooldown	18
17	Design of Wing Tank Simulator Chiller Plate	18

18	Height vs Temperature for Cooldown in the Wing Tank Simulator at Various Times Using the Chiller Plate	19
19	Flow Rate vs Temperature During Recirculation in the Wing Tank Simulator Using Five Different Fuels With the Vertical Arrows Showing the Location of the Measured Freeze Point +3°C Temperature for Each Fuel and the Vertical Black Line Showing the Jet A Specification +3°C Temperature (-37°C)	20
20	Two-Dimensional Geometries Representing the Boeing Tank, the Lockheed Tank, and the Three-Dimensional Geometry of the Wing Tank Simulator	23
21	Color Contour Plots Showing Simulated Temperature Profiles in the Lockheed Tank After 6 Hours and 7 Hours of Simulation	26
22	Measured and Calculated Temperature Profile Above the Tank Bottom Near the Tank Center for 6- and 7-Hour Cooling Periods for the Lockheed Experiment, With the Symbols Representing Measured Temperatures	27
23	Measured and Simulated Time-Varying Fuel Temperature 1.3 cm Above Lower Tank Surface in the Lockheed Tank, With the Symbols Representing Measured Temperatures	27
24	Two-Dimensional, Transient Simulations of Cooling of the Boeing Tank After 1 and 15 Minutes With Identical Upper and Lower Surface Temperatures and Buoyancy-Driven Flow	28
25	Measured and Simulated Fuel Temperature Distribution After 15 Minutes Above the Cooled Bottom Surface for Experiments Conducted by Boeing	29
26	Skin Temperature Schedule for FAA Test 30	30
27	Two-Dimensional Simulations of Cooling in the Wing Tank Simulator After 15 Hours for Vertical Walls of Uniform Temperature and Insulated Vertical Walls	30
28	Vector Plots Showing Flow in the Wing Tank Simulator After 15 Hours for Vertical Walls of Uniform Temperature and Insulated Vertical Walls	31
29	Measured and Simulated Temperatures for Uniform Wall Temperature or Adiabatic Boundary Conditions for Thermocouples Located 1.2 cm From the Sidewall or 1.3 cm Above the Bottom Wall, With the Symbols Representing Measured Temperatures	32
30	Skin Temperature Schedule for FAA Test 42	33
31	Dynamic Viscosity vs Temperature for Increases in Viscosity by Either 30% or 200% Relative to the Baseline Viscosity	34

32	Two-Dimensional, Time-Varying Simulations of the Fuel Temperature After 4 Hours of Cooling for the Baseline Fuel Viscosity, an Increase in Viscosity by 30%, and an Increase in Viscosity by 200%	35
33	Vertical Temperature Profile Near the Center of a Tank Compartment After 4 Hours of Cooling for Two Different Jet Fuels	36
34	Density vs Temperature for Changes in Density by $\pm 5\%$ From the Baseline Density	37
35	Transient Temperature Profile Above Lower Surface at the Vertical Centerline After 60 Minutes of Cooling for a Change of $\pm 5\%$ From the Baseline Density	37
36	Two-Dimensional Thermal Profile With Adiabatic Top Surface to Represent Ullage Space After 4 Hours of Cooling	38
37	Effect of the Ullage Space on the Fuel Temperature Profile Along the Vertical Centerline After 4 Hours of Cooling	39
38	Temperature Contours for Two-Dimensional Simulations After 40 Minutes of Cooling for a Full Tank or for Air Gap Heights of 3.8 cm and 26.5 cm	40
39	Measured and Calculated Temperatures From Two-Dimensional Simulations Near the Center of a Tank Compartment That Includes an Ullage Space, With the Symbols Representing Measured Temperatures	41
40	Three-Dimensional Unstructured Grid	42
41	Comparison of Temperature Color Contour Plots Within the Wing Tank Simulator Simulated by Three-Dimensional and Two-Dimensional Calculations	43
42	Temperature Measurements and Two- and Three-Dimensional Simulations at a Single Location for Different Times, With the Symbols Representing Measured Temperatures	43
43	Measured and Simulated Temperatures for a Tank With an Ullage Space, With the Symbols Representing Measured Temperatures	44

## LIST OF TABLES

Table		Page
1	Freeze Points of Jet A Fuels Studied in the Viscometer	6
2	Total Weight Percent Normal Alkanes in Fuels Studied	8
3	Descriptions of the Tests Performed in the Wing Tank Simulator	16
4	Fuel Properties for the Wing Tank Simulator	21
5	Select CFD Simulations	24
6	Grid Studies for Different Conditions	25

## LIST OF ACRONYMS

ATA	Air Transport Association
CFD	Computational fluid dynamics
CONUS	Continental United States
cP	Centipoise
CRC	Coordinating Research Council
cSt	centiStokes
DFSC	Defense Fuel Supply Center
FAA	Federal Aviation Administration
GC-FID	Gas Chromatography with Flame Ionization Detection
GC-MS	Gas Chromatography with Mass Selective Detection
gpm	Gallons per minute
U.S.	United States
VOF	Volume of fluids

## EXECUTIVE SUMMARY

United States commercial jet aircraft are currently limited to operating at measured wing tank fuel temperatures that are greater than 3°C above the fuel specification freeze point (-40°C for Jet A fuel and -47°C for Jet A-1 fuel). The recent opening of new, long-duration polar routes subjects fuel tanks to lower temperatures for longer periods. When the measured in-tank fuel temperature approaches these low-temperature limits, pilots are forced to modify flight path, altitude, and/or airspeed to raise these temperatures. Since many jet fuel samples have freeze points that are significantly lower than the fuel specification, airline companies would like to change the low-temperature operational limit to greater than 3°C above the measured freeze point of the particular fuel sample in the aircraft fuel tank. Such a change could minimize unnecessary flight path, altitude, and/or airspeed alterations, resulting in significant cost savings. This report provides the results of studies of low-temperature effects on jet fuel properties and fuel system operation. An aircraft wing tank simulator was designed and built that can be subjected to low temperatures inside an environmental chamber. The simulator employs actual Boeing 747 fuel hardware, such as a boost pump and flapper valves. The fuel flow rates, temperature profiles, pressures, and pump power are measured as a function of temperature. A series of laboratory studies were performed to better characterize fuel properties at these low temperatures. These included low-temperature scanning Brookfield viscometry measurements; normal alkane chromatographic analyses; and freeze, cloud, and pour point measurements. The results of this study show that increased fuel viscosity at these low temperatures resulted in significant reductions in flowability and pumpability. Fuels with low freeze point temperatures display increased viscosity near their freeze point relative to higher temperature freeze point fuels. The implications of these findings are likely fuel system dependent. A computational fluid dynamics study of the wing tank simulator was performed to allow prediction of fuel temperatures in real fuel systems. The computational results showed that the presence or absence of ullage space greatly affected fuel tank vertical temperature profiles. In addition, the results indicated the importance of the location of the fuel temperature sensors in obtaining accurate measurements of the lowest fuel temperatures in the tank.

## 1. INTRODUCTION.

Long-duration commercial aircraft flights are currently limited in altitude, speed, and/or route because of concerns with the cold ambient conditions causing fuel crystallization and/or reduced fuel flowability. Currently, aircraft are limited to operation under conditions where the measured in-tank fuel temperature is more than 3°C above the fuel specification freeze point. These specification freeze points are -40°C for Jet A fuel and -47°C for Jet A-1 fuel. Thus, commercial aircraft are currently limited to fuel temperatures of -37°C and -44°C for Jet A and Jet A-1, respectively. Many fuel samples exhibit freeze points that are significantly lower than the specification freeze point, as shown in figure 1, for fuel freeze points measured at North American airports. Airlines would like to use the actual measured freeze point of the fuel delivered to the aircraft, rather than the specification freeze point, for long-duration flights. Using the measured freeze point would permit lower fuel temperatures during flight operations, resulting in more flexibility in flight profiles. This increased flexibility in flight altitude, speed, and route may result in significant advantages for airlines and their customers, including lower ticket prices and greater flight availability.

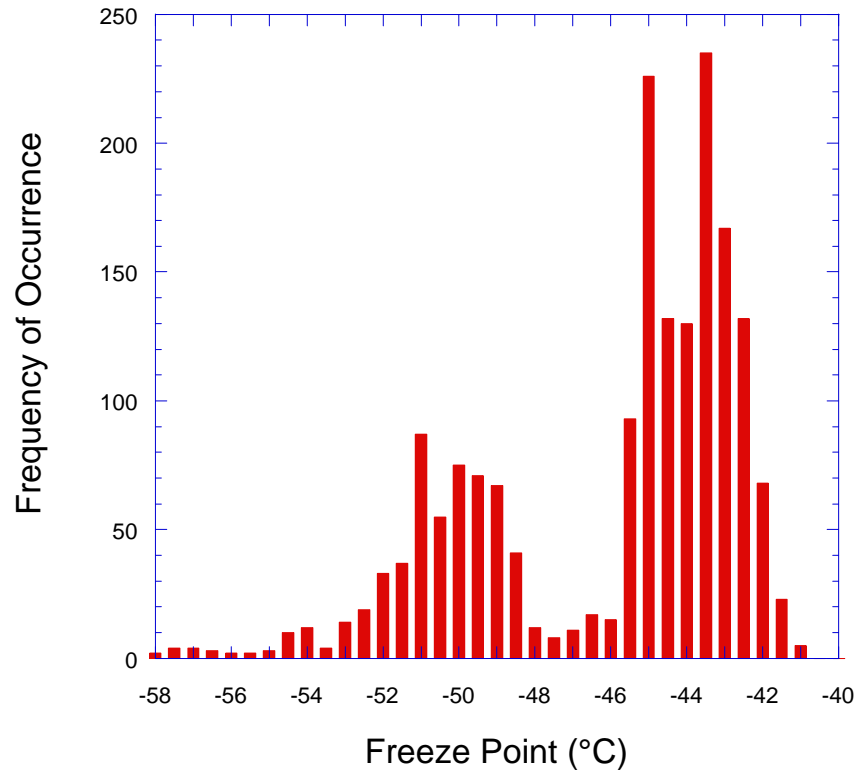


Figure 1. Frequency of Occurrence of Fuel Freeze Points for Jet A Fuels (Specification Freeze Point -40°C max) Measured at North American Airports (data courtesy of Francis Davidson, Phase Technology)

The goal of this study was to determine if aircraft fuel system function would be negatively impacted by operation at these lower fuel temperatures. ASTM D 2386 defines the freeze point as the temperature at which all visible crystals have melted after heating previously frozen fuel, which dictates that fuel above its measured freeze point consists of a single liquid phase. Thus,

no crystallization or solidification would be expected during operation above the measured freeze point, as long as the measured in-tank fuel temperature accurately represents the lowest temperature in the fuel system. It is essential to evaluate the measurement of fuel temperatures within aircraft fuel systems. Fuel crystallization begins when the fuel temperature reaches the cloud point [1]. At this temperature, the largest normal alkane species present in the fuel (typically n-C<sub>17</sub> to n-C<sub>19</sub>) begins to form orthorhombic crystals (figure 2) [2]. Figure 3, a gas chromatogram of a Jet A fuel, shows the range of typical normal alkane species present. As the temperature is further lowered, these crystals begin to form an interlocking network that inhibits fuel flow [3]. Below the pour point temperature, the fuel no longer flows freely and is unavailable to the aircraft engines.

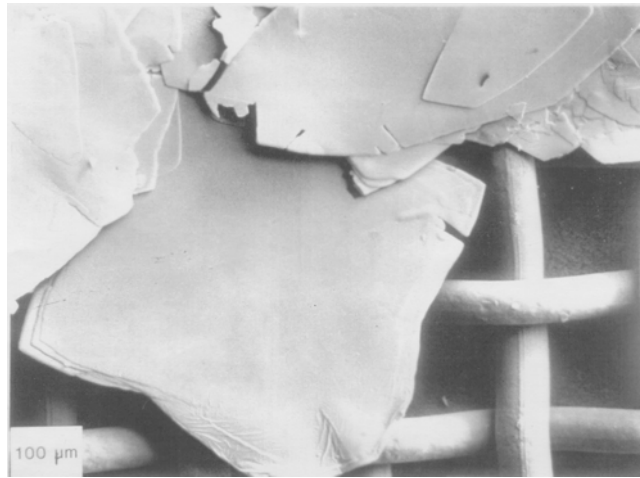


Figure 2. Scanning Electron Micrograph of Normal Alkane Crystals (Courtesy of R.D. Tack, Infineum UK Ltd.)

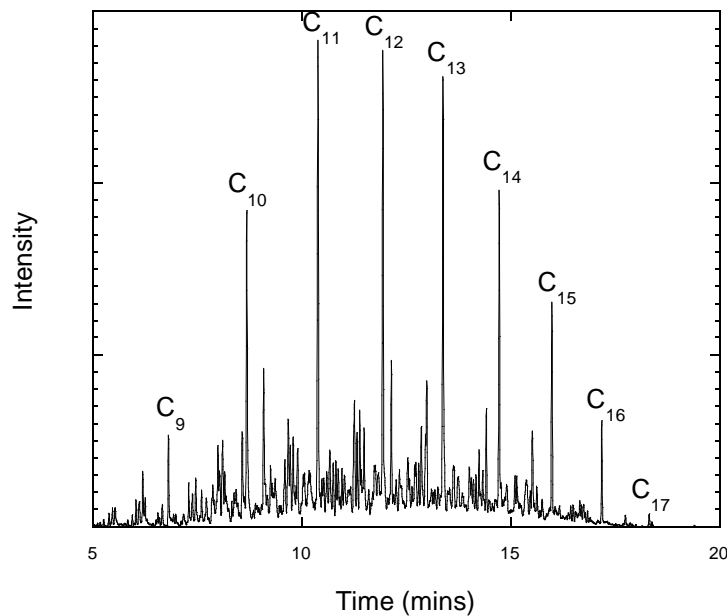


Figure 3. Chromatogram of a Jet A Fuel Showing the Normal Alkane Distribution

Despite the fact that a single phase is expected above the freeze point, other fuel properties need to be examined at these lower temperatures to evaluate their impact on flight operation. In particular, the fuel viscosity is an important parameter for correct operation of fuel systems. Fuel must exhibit a low enough viscosity to flow readily through narrow fuel lines, screens, and valves and to be pumped from the fuel tanks to the engine. Also, high fuel viscosity can interfere with proper fuel atomization in combustor nozzles and proper ignition in the combustor. This is especially crucial for engine relight at altitude. Thus, it is essential to evaluate the effect lower fuel temperatures will have on fuel viscosity and aircraft or engine operation.

Aircraft fuel tanks usually contain temperature sensors that provide the crew with limited information on the fuel temperature within a subset of the aircraft fuel tanks. A single sensor within a wing tank is unable to provide information on the range of temperatures throughout the tanks. Previous measurements in fuel tank simulators have shown a significant variation in the fuel vertical temperature profile (figure 4) [4]. Such data show that single-location fuel temperature measurements in wing tanks can provide incomplete and misleading temperature information to the crew. In particular, sensors located near the vertical midpoint of the tank may only measure the relatively high temperatures in this location, while temperatures may be considerably lower near the lower and upper skins. Thus, it is important to better understand the heat transfer within aircraft wing tanks so that fuel temperatures can be more realistically predicted.

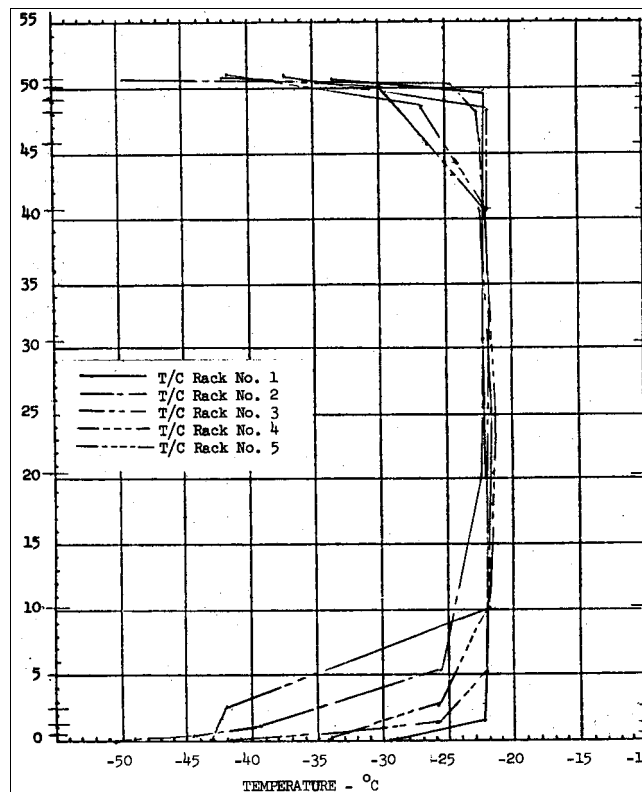


Figure 4. Lockheed Data Showing Vertical Temperature Profiles at Various Locations in a Wing Tank Simulator [4]

Results are presented here on studies performed on the effect of temperature on the flowability and pumpability of low-temperature fuel. In particular, results are presented on three main areas of research: (1) laboratory measurements of jet fuel chemical and physical properties, (2) measurements of low-temperature fuel flowability in a wing tank simulator, and (3) computational fluid dynamics (CFD) techniques for the prediction of fuel tank temperature profiles. The laboratory measurements of chemical and physical properties include viscosity measurements of jet fuels as a function of temperature; analyses of the normal alkane concentrations of fuels; and freeze, cloud, and pour point measurements of fuel mixtures. These studies are detailed in the following sections.

## 2. LABORATORY STUDIES.

Laboratory studies were conducted to obtain fundamental information on the effect of low temperatures on fuel properties and behavior. Scanning Brookfield viscosity studies were performed to measure the effect of temperature on fuel viscosity and flowability. These studies also provided insight into the flow behavior observed in the wing tank simulator. Quantitative analyses of the fuel's normal alkanes were obtained by gas chromatography. These studies provided information on how differences in the chemical composition of various fuel samples affect low-temperature fuel properties. In addition, freeze, cloud, and pour point analyses of binary mixtures of fuel samples were obtained via a Phase Technology Petroleum Analyzer. These studies explored possible concerns in estimating the freezing behavior of binary fuel mixtures, with respect to the mixing of fuel samples that occurs during aircraft refueling.

### 2.1 SCANNING BROOKFIELD VISCOMETRY.

Viscosity is one of the most important fuel properties to consider when studying the effect of temperature on fuel flowability and pumpability. Viscosity is a measure of the resistance to flow of a fluid. The specification for Jet A and Jet A-1 fuels, ASTM D 1655, requires a maximum viscosity of 8.0 centiStokes (cSt) measured at  $-20^{\circ}\text{C}$ . The viscosity specification was designed to assure adequate fuel flow through fuel lines, valves, and pumps at reduced temperature. In addition, the viscosity specification also assures proper fuel atomization in engine combustors. The performance of combustor nozzle atomizers, as well as subsequent proper fuel evaporation and mixing with air, are strongly dependent on the fuel viscosity. Engine manufacturers usually specify a maximum fuel viscosity of 12 cSt at the nozzle to assure reliable engine-starting performance. The standard viscometry technique used for specification measures kinematic viscosity by measuring the time required for a fixed volume of fuel to flow through a calibrated capillary tube. This test is performed at the desired fixed temperature. In the present studies, the dynamic viscosity was measured via a Scanning Brookfield Viscometer. This technique has the capability to rapidly measure viscosity as a function of temperature. Such measurements would be extremely time consuming and/or impractical using the capillary tube technique.

Viscosity measurements were performed using a Tannas Scanning Brookfield Plus Two Viscometer. As the fuel sample (30 mL) is cooled from  $-40^{\circ}$  to  $-65^{\circ}\text{C}$  at  $5^{\circ}\text{C}/\text{hour}$ , the viscosity is measured continuously by the increasing torque generated by a spindle rotating in the fluid at constant speed (12 rpm) [1]. The scanning Brookfield viscosity measurements over a range of temperatures are anchored at  $-40^{\circ}\text{C}$  by calibrating to measurements obtained at the same temperature using ASTM D 445, which measures the time for a volume of liquid to flow under

gravity through a calibrated glass capillary viscometer. The  $-40^{\circ}\text{C}$  fuel density is estimated to be  $0.85\text{ g/mL}$  from estimated data in the Coordinating Research Council (CRC) Handbook of Aviation Fuel Properties [5]. Cloud, pour, and freeze point data were acquired using a Phase Technology PSA-70V Petroleum Analyzer, via ASTM D 5773, D 5949, and D 5972, respectively. The pour point analyses were conducted at  $1^{\circ}\text{C}$  intervals. The freeze and cloud point analyses have uncertainties of  $\pm 1^{\circ}\text{C}$ , while the pour point analyses have uncertainties of  $\pm 3^{\circ}\text{C}$ .

Figure 5 shows plots of viscosity versus temperature using the scanning Brookfield technique. This technique measures dynamic viscosity rather than kinematic viscosity as in the ASTM D 445 method. The dynamic viscosity ( $\eta$ ) can be related to the kinematic viscosity ( $\nu$ ) via the density ( $\rho$ ) by,  $\eta = \nu\rho$ . The nine fuels shown are all Jet A fuels, which were chosen for their wide range of freeze points (table 1). The figure shows that the fuels display a very slow rise in viscosity as they are cooled below  $-40^{\circ}\text{C}$ . Upon further cooling, the fuels display a relatively sudden, rapid increase in viscosity. Previous work has shown that this sudden, rapid rise in viscosity occurs very close to the measured cloud point and that microscopic crystal formation begins at this temperature [1]. These observations support the conclusion that this increase in viscosity is due to the occurrence of solid crystal formation in the fuel, as the cloud point is the temperature at which visible solids are first observed upon cooling. For the current study, the primary interest was how the liquid-phase viscosity varies with temperature. To better show this variation, portions of the viscosity data in the crystallization regime (i.e., the high viscosity regime) have been omitted, and the remaining data rescaled and replotted using this liquid-phase only data (figure 6) for the nine Jet A fuel samples.

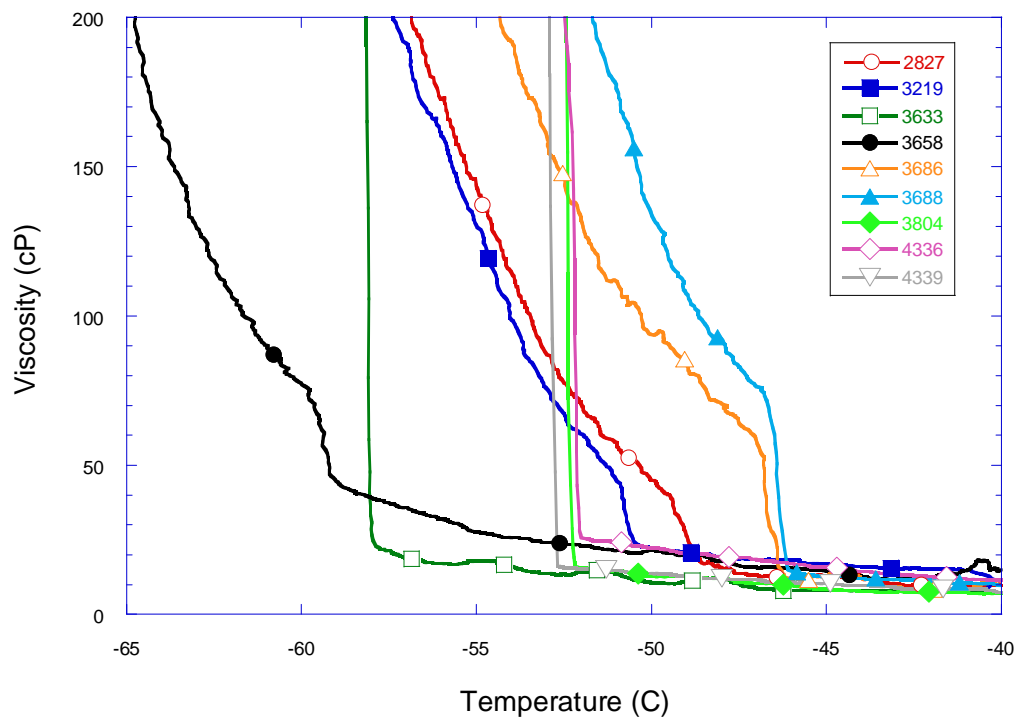


Figure 5. Measured Viscosity vs Temperature for Nine Jet A Fuel Samples

Table 1. Freeze Points of Jet A Fuels Studied in the Viscometer

Fuel Sample Identification	Freeze Point (°C)
3688	-41.6
3686	-41.9
2827	-42.9
3219	-46.4
4336	-47.2
3804	-47.6
4339	-48.6
3658	-53.1
3633	-55.1

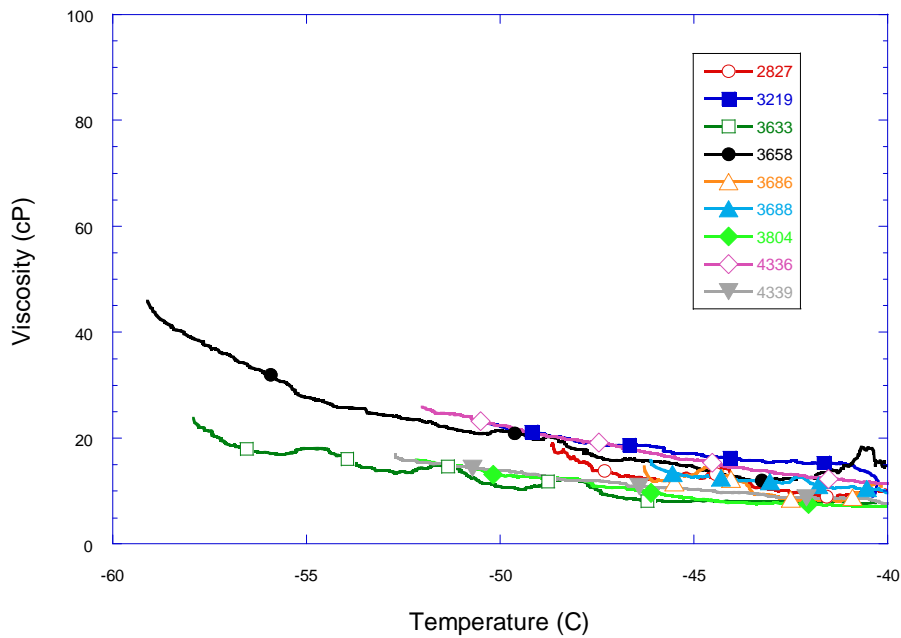


Figure 6. Viscosity vs Temperature for the Liquid-Phase Region for Nine Jet A Fuel Samples

Figure 6 shows how the liquid-only viscosity changes with temperature over a range of jet fuel samples. The figure shows that, in general, there is a gradual rise in viscosity over this temperature range. More interestingly, it is apparent that fuels with relatively high cloud/freeze points have relatively low viscosities at their cloud/freeze point, while fuels with low cloud/freeze points have relatively high viscosities at their cloud/freeze point (the cloud point is near the lowest viscosity measurement for each fuel). These results have important implications for fuel system operation. The results show that there may be issues in using the fuel freeze point (which is usually 2° to 6°C above the cloud point) to evaluate fuel flowability. For example, the low-temperature freezing fuel 3658, which has a freeze point of -53.1°C and a

cloud point of  $-59.2^{\circ}\text{C}$ , displays a viscosity of 46.4 cP at its cloud point, while fuel 3688, which has a freeze point of  $-41.6^{\circ}\text{C}$  and a cloud point of  $-46.1^{\circ}\text{C}$ , has a viscosity of 11.7 cP at its cloud point. This factor-of-four difference in viscosity may have a significant effect on fuel flowability and pumpability at these temperatures. Despite these differences near their cloud point temperatures, these two fuels display very similar viscosities in the temperature range  $-40^{\circ}$  to  $-45^{\circ}\text{C}$ . The significance of this factor-of-four difference in viscosity will depend on the specific fuel system requirements, such as required flow rate for the engines and the ability of the fuel system pumps to handle higher viscosity fuel. This observation of increased viscosity near the freeze point of lower freeze point fuels relative to high freeze point fuels is an important issue to consider when deciding whether to use low freeze point fuels at temperatures below the specification freeze point. These data show that it is important to consider the effect that this increase in viscosity will have on fuel flow to the engine and on fuel atomization in the combustor. Studies performed in the wing tank simulator further elucidate how low temperatures affect viscosity and the resulting fuel flowability and pumpability in actual fuel system components. Additional insight into these results will be obtained via normal alkane analyses of the fuels.

## 2.2 NORMAL ALKANE MEASUREMENTS.

Jet fuels consist of mixtures of hundreds or thousands of different species. These primarily consist of alkanes (normal, branch, and cyclic) and aromatics (alkyl-substituted benzenes). Previous work has shown that normal alkanes are the first species to crystallize upon fuel cooling [6]. Crystallization of only a small fraction ( $<1\%$ ) of the species present is enough to cause fuel gelation and prevent flow [7 and 8]. While low-temperature fuel behavior is a strong function of the overall normal alkane profile, the largest normal alkanes crystallize most readily and thus have the greatest effect in determining low-temperature properties near the freeze and/or cloud point. Normal alkane analyses have been performed on a range of jet fuels to provide information on how the normal alkane profile contributes to low-temperature fuel flowability.

Normal alkane analyses of the fuels studied were performed via a combination of gas chromatography with flame ionization (GC-FID) and mass spectrometric (GC-MS) detection. The  $\text{C}_7$  to  $\text{C}_{16}$  normal alkanes were quantified by GC-MS. An average response factor calibration was generated by measuring at least five concentrations of  $\text{C}_7$  to  $\text{C}_{16}$  external standards, with nonadecane ( $\text{n-C}_{19}\text{H}_{40}$ ) as an internal standard. Each fuel sample was diluted into the concentration range of the calibration and spiked with the internal standard at the same concentration as in the calibration standards. The  $\text{C}_{17}$  to  $\text{C}_{19}$  normal alkanes were quantified by GC-FID. Several concentration levels of  $\text{C}_{17}$  to  $\text{C}_{19}$  external standards were analyzed, and a calibration curve was generated using linear regression. These analyses were performed at a lower dilution to enable more accurate quantization of these larger normal alkanes.

The results of the normal alkane analyses are shown in figure 7, and the total normal alkane content of each fuel is shown in table 2. Previous work has shown that the larger normal alkanes species present in each fuel are responsible for incipient crystallization as fuel is cooled to temperatures near the cloud point [1, 6, and 9]. It is instructive to compare the normal alkane distributions of the fuels studied to seek the cause of the observed higher viscosity and lower flowability of lower freeze point fuels relative to higher freeze point fuels near their respective freeze points. Careful study of figure 7 shows that fuels that have the highest concentrations of

the largest normal alkanes ( $C_{16}$  to  $C_{19}$ ), such as fuels 3686 and 3688, also have the highest freeze points (see table 2). Also, fuels that have the lowest concentrations of these large normal alkanes, such as fuels 2976 and 3633, have the lowest freeze points. Such observations show how the concentration of the larger normal alkanes influences freeze point.

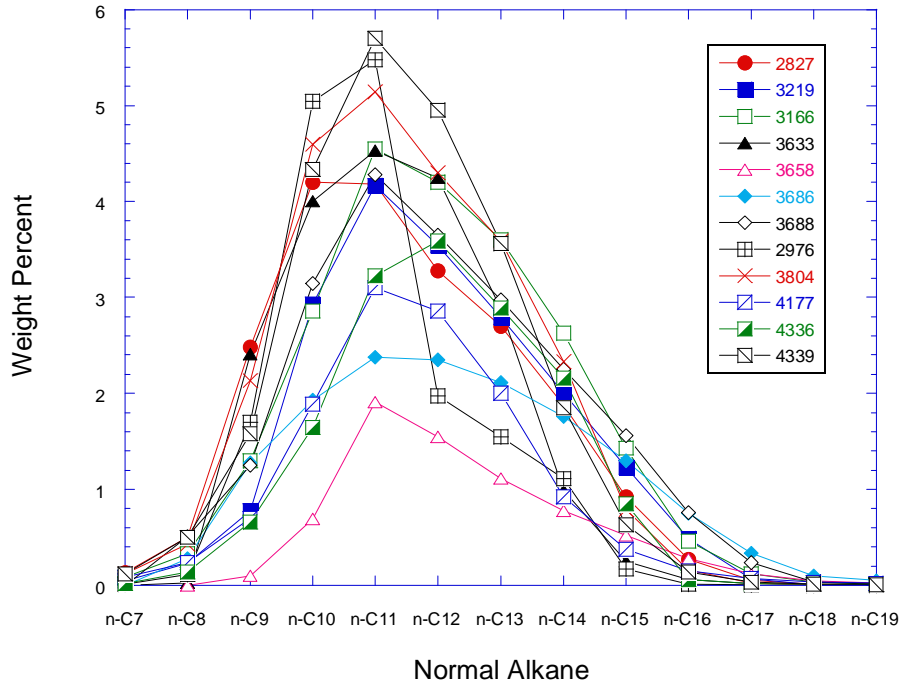


Figure 7. Weight Percent of the Normal Alkanes for the 12 Fuels Studied

Table 2. Total Weight Percent Normal Alkanes in Fuels Studied

Fuel and Type	Total Weight Percent Normal Alkanes
3658 Jet A	7.1
4177 JP-8	12.3
3686 Jet A	14.6
4336 Jet A	15.2
2976 JPTS	17.2
3219 Jet A	18.3
3633 Jet A	19.4
2827 Jet A	20.6
3688 Jet A	20.7
3166 Jet A	21.6
4339 Jet A	23.4
3804 Jet A	23.6

It is interesting to consider why lower freeze point fuels have higher viscosities near their freeze point than do high freeze point fuels, as observed in section 2.1. One possible explanation relates to the ideality of the jet fuel mixture in the liquid phase versus the solid phase. It is known, in the temperature region in which crystallization begins, that the incipient solid crystals consist of highly nonideal solid solutions of the larger normal alkanes (such as C<sub>16</sub> to C<sub>19</sub>) present in the fuel [10]. These large normal alkanes make up only a small fraction of the total normal alkane concentration (e.g., see figure 7). In contrast, the remaining liquid fuel displays mixture properties that are very close to ideal. Thus, the crystallization of larger normal alkanes from the fuel, and therefore the freeze point, is highly dependent on the concentration and identity of these species. The liquid mixture should display ideal mixture viscosity behavior, with the resulting viscosity being a function of the bulk of the species present. Of the species present in jet fuel, the normal alkanes are thought to contribute to the viscosity to the largest extent. Thus, the viscosity is mostly a function of the overall distribution of the normal alkanes in the fuel, while the freeze point is more dependent on the distribution of the largest normal alkane species. Therefore, if two fuels differ only in the concentration of the larger normal alkanes, the one with the higher level of large normal alkanes will exhibit a higher temperature freeze point. Since the distribution of the remaining smaller normal alkanes remain the same, these fuels should have similar viscosities. However, the lower freeze point fuel will crystallize at lower temperatures, where the liquid viscosity will be higher than that of the higher freeze point fuel at its freeze point. Thus, the observation that lower freeze point fuels display higher viscosities near their freeze points likely results from the fact the viscosity is mostly a function of the overall normal alkane distribution, while freeze point is more sensitive to the concentration of the larger normal alkanes present.

### 2.3 STUDIES OF THE INTERMINGLING OF FUELS.

It is important to assess the effect of the mixing of fuel samples on the freezing characteristics of fuel because of the frequent occurrence of mixing during aircraft operation. Mixing can occur in numerous storage and pipeline locations after the fuel leaves the refinery. Most importantly, the mixing of fuel samples almost always occurs during aircraft refueling. Aircraft are typically refueled without defueling the remaining fuel from the previous flight. Thus, the “new” refueled fuel is mixed with varying amounts of “old” fuel. Ideally, the blending of two fuel samples with different freeze points will yield a mixture that exhibits a freeze point between the two samples, with a linear relationship between the mixture fraction and freeze point (figure 8). But fuels do not necessarily form ideal mixtures, and nonideal behavior has been previously observed [11 and 12]. The least desirable nonideal behavior is when the intermingling of two fuels produces a mixture that has a higher freeze point than either of the two starting fuels, as shown hypothetically in figure 9. Such behavior has been observed previously [11], although the increase in freeze point of these mixtures above the ideal linear dependence was always less than 2°C and usually less than 1°C. If this behavior is found to commonly occur, then using the measured freeze point +3°C as an operational limit is complicated by being unable to predict the actual fuel mixture freeze point upon refueling. Thus, a series of fuel mixtures have been studied to evaluate the behavior of freeze point on mixture fraction. Studies have concentrated on mixtures of fuels with very different freeze points so that any measured nonlinearity or nonideal behavior would be readily apparent (i.e., nonlinearity greater than the experimental reproducibility).

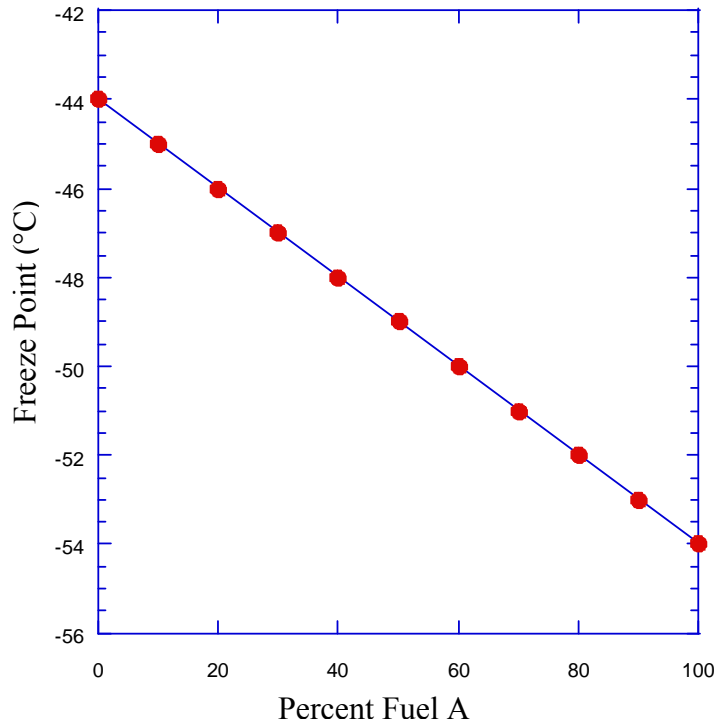


Figure 8. Hypothetical Ideal Mixture Freeze Point Behavior for the Mixing of Two Fuels (Fuel A, Freeze Point -54°C and Fuel B, Freeze Point -44°C)

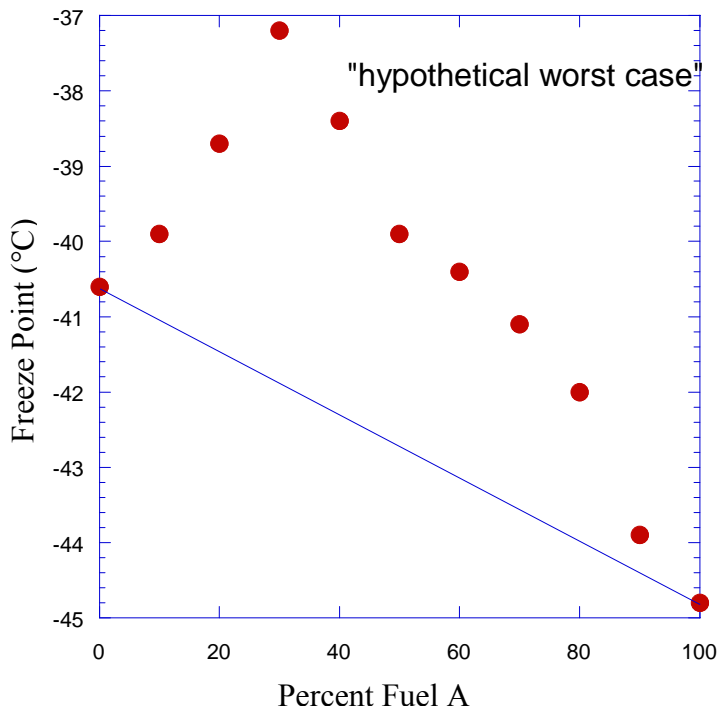


Figure 9. Hypothetical Mixture of Two Fuels With the Mixture Producing a Fuel With a Higher Freeze Point Than the Original Fuels

The intermingling of fuels was studied using freeze point measurements obtained on the Phase Technology Petroleum Analyzer. Examples of the various behaviors obtained for fuel mixtures are shown in figure 10. The most common behavior observed on mixtures of two fuels is shown in figure 10. These Jet A fuels were selected because of their extreme freeze points (see figure 1, for example). Fuel 3686 has a freeze point near  $-42^{\circ}\text{C}$ , while fuel 3633 has a freeze point near  $-55^{\circ}\text{C}$ . The results show a near linearity for the full range of the blended fuels. The figure shows that there may be some nonlinearity at the dilute blends of both fuels (i.e., a slight “S” shape curve to the data). These very dilute blends ( $<20\%$  of added fuel) appear to have freeze points closer to that of the fuel being diluted (i.e., the fuel in higher concentration). The linear mixture approximation always yields a freeze point within  $1^{\circ}\text{C}$  of the measurement for mixtures of these two fuels with very different freeze points.

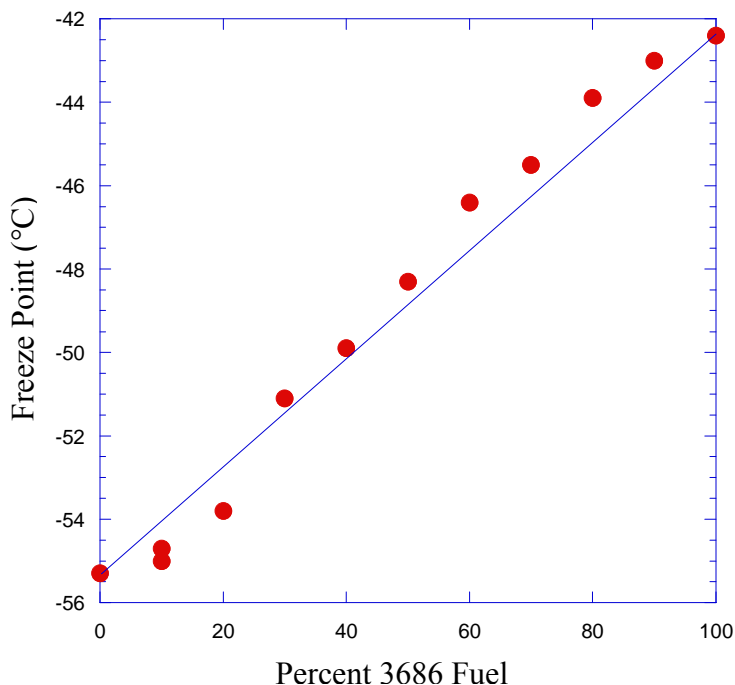


Figure 10. Freeze Points for Mixtures of Two Fuels, 3686 and 3633, Showing Near Linear Behavior

Next, a mixture that displays behavior that is markedly nonlinear was discovered. These results are shown in figure 11. Fuel 3775 is a JPTS specification fuel, which displays a freeze point near  $-54^{\circ}\text{C}$  (the JPTS freeze point specification is  $-53^{\circ}\text{C}$  max). Fuel 3686 is a Jet A fuel, with a freeze point near  $-42^{\circ}\text{C}$ . These fuels have very different freeze points, and they might be used to represent the maximum difference that could be encountered in commercial flight operations. The figure shows that adding relatively small amounts of 3775 fuel to 3686 fuel decreases the freeze point in a linear way. Thus, adding the low-freezing fuel to the high-freezing fuel decreases the freeze point. On the other hand, adding small amounts of 3686 fuel to 3775 also decreases the freeze point slightly (about  $1^{\circ}\text{C}$  at 20% 3686). This result shows the complex behavior observed upon the mixing of fuels. This type of behavior is reminiscent of the colligative freeze point depression observed upon the mixing of pure components [13]. The data

points shown in the figure are averages of two or three measurements. The error bars are one sigma standard deviation. Interestingly, the error bars become quite large near the break in linearity observed at 70% of the 3775 fuel. Thermodynamic modeling of the freeze point of fuel and fuel-like mixtures could yield insight into the cause of this nonlinear behavior [10 and 14].

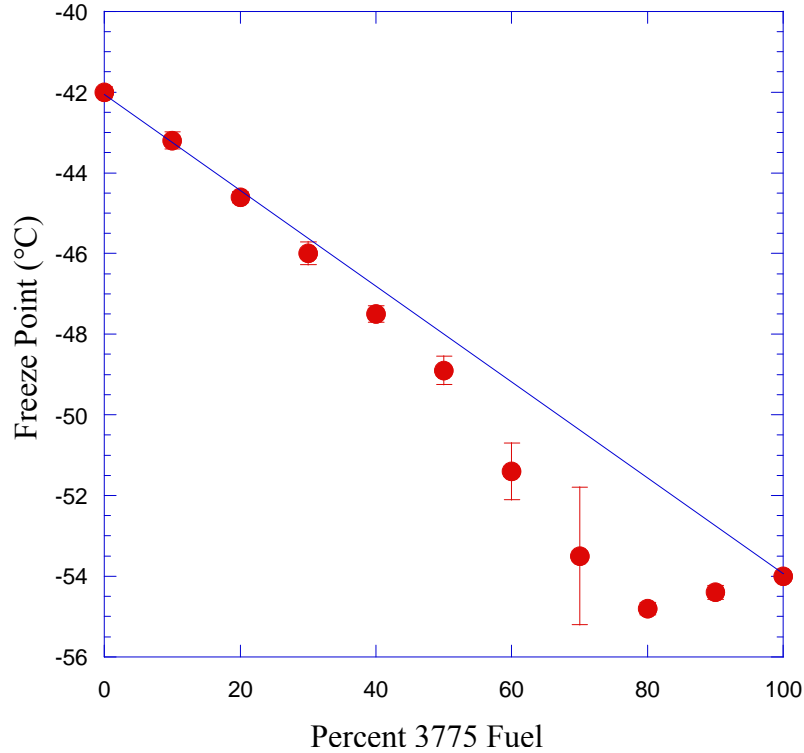


Figure 11. Measured Freeze Point vs Percentage of Fuel 3775 in Mixtures of Fuel 3775 With Fuel 3686 Showing Nonlinear Behavior

Figure 11 shows that the actual freeze points of the mixtures is lower than that predicted by a linear interpolation between the freeze points of the individual fuels. This behavior is desirable when using calculational techniques for predicting the freeze points of fuel blends, such as that used by Air Canada and Boeing (Boeing Service Letters 747-SL-28-98 and 767-SL-28-9). These letters detail a technique to predict the freeze point of mixtures of Jet A and Jet A-1 fuels based upon the mixture fraction and the specification freeze points. The opposite type of behavior, where the freeze point is greater than that predicted by linear extrapolation has been observed by Phase Technology [11]. The behavior observed by Phase Technology is worrisome, because it implies that when two fuels are mixed, a third fuel can be created that can have a higher freeze point that is higher than the two by some unknown amount.

The measurements shown above were on fuels that had significantly different freeze points. Results on two fuels with very similar freeze points are shown in figure 12. Fuel 3775 is a JPTS specification fuel and fuel 3633 is a Jet A fuel with a very low freeze point. The figure shows that there is only a three-degree difference in freeze point between these two fuels. The data obtained at various mixing ratios appear quite noisy due to the small difference in freeze point

between the two fuels. No apparent nonlinearity is observed in these fuels within the experimental uncertainty.

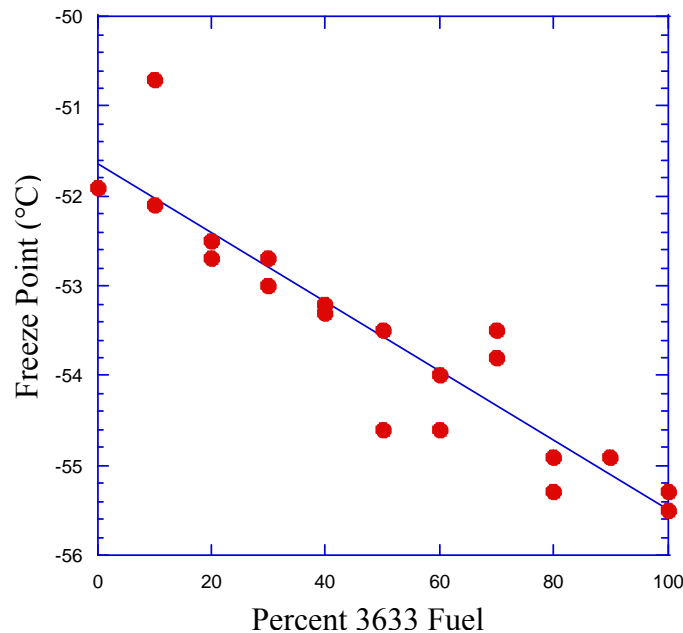


Figure 12. Measured Freeze Point vs Percentage of Fuel 3633 in Mixtures of Fuel 3775 With Fuel 3633

This brief study of the effect of mixture fraction of binary fuel mixtures on freeze point demonstrates that nonlinearity of freeze point versus mixture fraction is commonly observed. Theoretically, this nonlinearity can yield mixtures that display freeze points below and above the linear mixture approximation. Mixtures that display freeze points at higher temperatures than the linear approximation have not been observed in the present work, although only a limited number of mixtures were studied. Such mixtures are highly undesirable if linear behavior is assumed, as it results in fuel with a higher freeze point than expected. It is important to better understand the behavior of freeze point on mixture fraction because fuel mixtures are commonly formed upon aircraft refueling. In particular, it is important to understand when positive and negative deviations from nonlinear behavior occur. It is also important to find the fuel mixture components and/or combinations of components that result in nonlinear behavior. Further studies of binary mixtures of fuel and fuel-like components along with thermodynamic modeling of fuel solidification could be beneficial.

### 3. WING TANK SIMULATOR STUDIES.

As long as the measured in-tank fuel temperature accurately represents the lowest temperature in the fuel system, aircraft fuel system operation at temperatures above the measured freeze point dictates that fuel at these temperatures will consist of a single liquid phase. As mentioned above, the important concern is that the fuel viscosity remains low enough to be pumpable by the fuel system pumps and flow at high enough flow rates to supply the required fuel to the engines. The previous fuel tank simulator work by Boeing and Lockheed concentrated on temperatures

significantly below the fuel freeze point where two phases were expected, i.e., a liquid and solid phase [4 and 15-20]. In these studies, which concentrate on conditions above the measured fuel freeze point, it is important to test fuel system components that are involved in delivering the fuel at the maximum flow rate needed by the engines. Such components include items with tight passageways including flapper valves, narrow tubes, screens, and most importantly, the fuel boost pump. The goal was to design and build a system that tests the pumpability through actual fuel system components.

Currently, one of the most commonly used aircraft for long-duration commercial flight is the Boeing 747-400. Thus, most of the simulation work has been directed toward this ubiquitous aircraft. Figure 13 shows the location of the fuel tanks in the aircraft. Fuel in the outboard main tanks (Numbers 1 and 4) are subjected to the coldest temperatures because these tanks are not used until near the end of the typical flight. Thus, fuel in these tanks is subjected to cold temperatures for the longest duration. Additional drawings and photographs of the Boeing 747 fuel system and wing tanks are shown in appendix A.

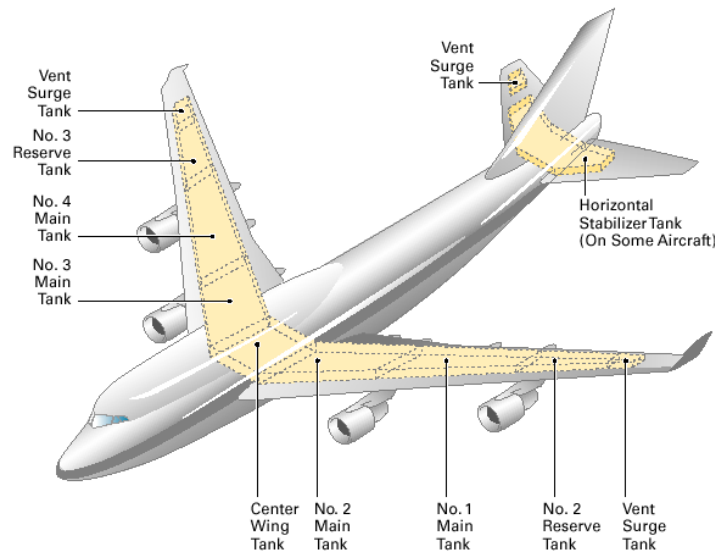


Figure 13. A Boeing 747 Showing Location of Fuel Tanks

To better understand the effect of low temperatures on the Boeing 747 fuel system, a wing tank simulator, including actual Boeing 747 fuel system components, was constructed. The simulator was designed to run under conditions similar to those found in the aircraft wing tank during a long-duration flight. Figure 14 shows a simplified drawing of the aluminum fuel tank and internal components that were used for the experimental simulations. A photograph of the wing tank simulator is shown in figure 15 and additional photographs are shown in appendix B. The entire tank is contained within an environmental chamber (Tenney Environmental, Model T64C15SPL). The chamber can provide minimum temperatures of  $-73^{\circ}\text{C}$ . The chamber is sufficient to produce a low-temperature environment similar to that expected for aircraft flying at high altitudes for long periods. For safety concerns, the environmental chamber is purged with nitrogen, and nitrogen (rather than air) resides in the fuel tank ullage space. The pressure within

the fuel tank is maintained at ambient pressure. The major dimensions of the fuel tank (approximately 75 x 50 x 50 cm) provide a tank volume of 190 liter. The tank contains two chambers with a separating baffle rib and two 3-inch-high stringers that have elliptical 1.25" "limber" holes to allow fuel flow between the stringer-divided sections. In addition, there are three Boeing 747 flapper valves on the baffle, which is located between the two chambers. A single pump (Hydro-Aire, Model 60-98976-2, see appendix C), used for each engine in the Boeing 747-400, is powered by a Hobart/AXA 2200, 40 Hz, 115/200V, 7.5 kVA frequency converter/power supply. Also installed is a 16-mesh screen in the boost pump inlet, which is significantly finer and, thus, a more conservative test than the 4-mesh screen used in the inlet of the Boeing 747 aircraft. The top of the tank is closed with a plexiglass plate. The simulator is designed so that the fuel can be gravity drained, pumped out via the boost pump, or recirculated through the boost pump back to the tank through a "piccolo" return tube. A complete list of runs performed in the wing tank simulator is shown in table D-1 of appendix D. The types of tests performed in the wing tank simulator are summarized in table 3.

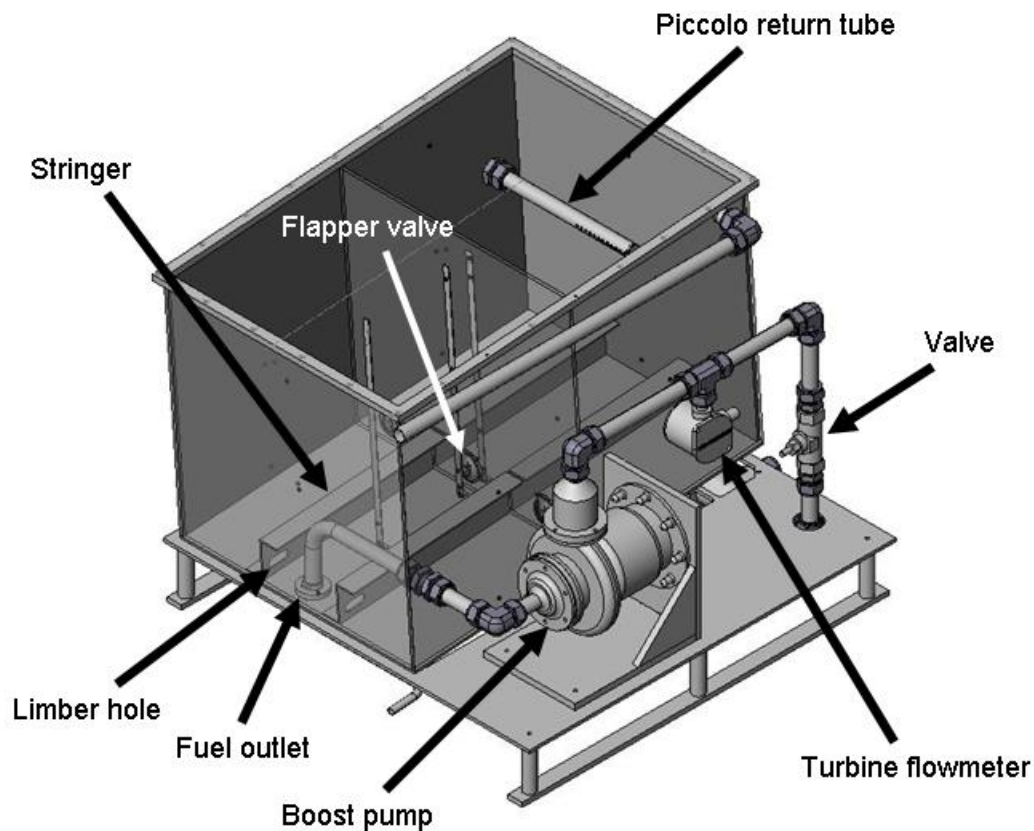


Figure 14. The Wing Tank Simulator

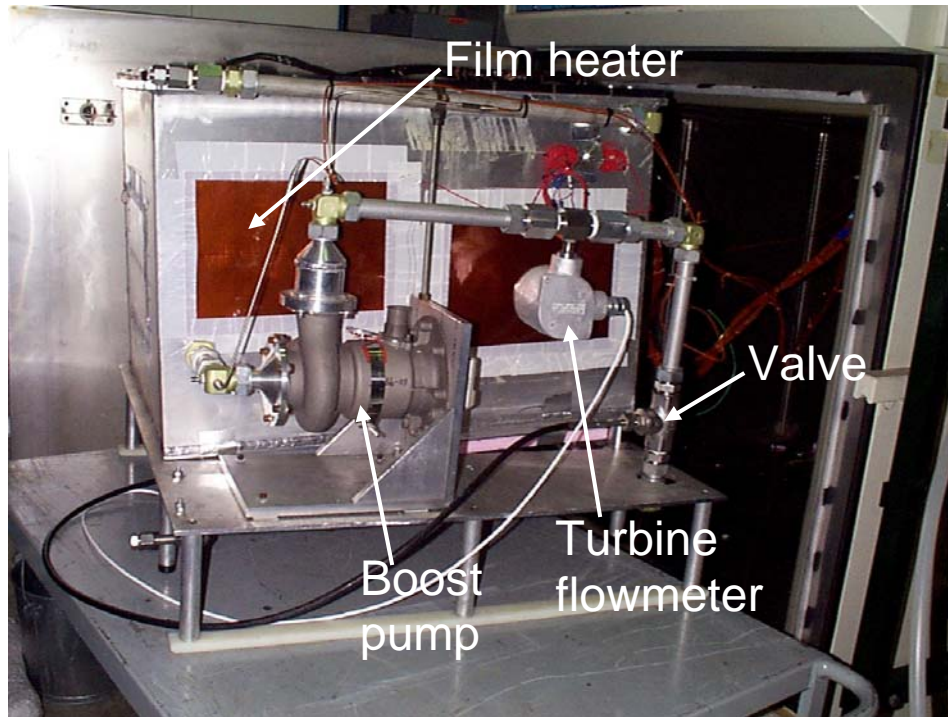


Figure 15. Wing Tank Simulator Showing Boost Pump, Turbine Flowmeter, Valve, and Film Heaters

Table 3. Descriptions of the Tests Performed in the Wing Tank Simulator

<p>Calibration and Check Out</p> <p>These initial tests were performed to check for proper functioning systems, including proper flow rate measurements, pressure measurements, pump power measurements, temperature measurements, checking for leaks, software and data acquisition system tests, and proper pump operation.</p>
<p>Recirculation</p> <p>In these tests, the fuel was cooled down (typically overnight) to a target temperature (usually a temperature slightly below the measured freeze point of the fuel). When the target temperature was reached, the pump was started and the fuel recirculated back to the tank through the piccolo tube. The fuel gradually heated up due to heat input from the pump. Recirculation continued until the fuel temperature reached the high temperature target, usually <math>-37^{\circ}\text{C}</math>. The fuel recirculation typically lasted 1 to 2 hours. Data were typically recorded at 10-minute intervals during cooldown and 1-second intervals during recirculation.</p>
<p>Pump Out</p> <p>Typically, pump-out tests were performed after a recirculation test was completed. The fuel was cooled over the course of several hours to the target temperature. The pump was then started and the flow directed to a vessel located outside the environmental chamber. At typical flow rates, it takes only about 2 minutes to empty the tank. Data were typically recorded at 1-second intervals.</p>

Table 3. Descriptions of the Tests Performed in the Wing Tank Simulator (Continued)

<p>Cooldown Only</p> <p>In cooldown-only tests, the fuel was cooled from ambient temperature to a given target temperature while monitoring fuel and tank temperatures without flow. Data were typically recorded at 10-minute intervals.</p>
<p>Temperature Flow Limit</p> <p>In temperature flow limit tests, the fuel was cooled to a target temperature (typically below the freeze point), and the pump was started for recirculation. If the fuel flowed successfully at this temperature, the fuel pump was stopped and the fuel cooled to a lower temperature, usually approximately 1°C lower. This process continued until proper fuel flow and pump operation was impeded due to the beginning of fuel solidification. Data were typically recorded at 1-second intervals during recirculation.</p>
<p>Low Flow</p> <p>In low-flow tests, recirculation tests were performed with the simulator valve set to provide a flow-reduced flow rate of 11 gallons per minute (gpm). These reduced flows will more closely simulate fuel flow during cruise conditions.</p>

The wing tank simulator was instrumented with a series of 48 thermocouples, a flow meter, and absolute and delta pressure gauges. Vertical temperature profiles were obtained at three locations in the tank. A post was located near the center of each of the two internal chambers (created by the single baffle rib—see appendix B) for mounting the thermocouples. A third post was mounted near a side wall to obtain boundary temperatures. Thermocouples were also mounted on the inside side walls and inside bottom surface of the tank. A thermocouple was located on the boost pump housing to measure the pump temperature. Thermocouples were also located in the pump inlet and outlet flows to measure the fuel temperature rise due to pump operation. A turbine flow meter was located downstream of the pump. Absolute and delta pressure gauges were located on the pump inlet and outlet. Pump power measurements could be obtained from current and voltage measurements of the three-phase power supplied to the pump. Thermocouple, flow, and pressure measurements were obtained at 10-minute intervals during cooldown and at 1-second intervals during pump operation.

Figure 16 shows temperature profiles obtained during initial cooldown studies in the wing tank simulator. Figure 16(a) shows that cooling the fuel down to -40°C takes over 15 hours. The figure also shows that the temperatures are nearly identical at three vertical locations above the bottom surface. Figure 16(b) shows that near the beginning of the cooldown period, the fuel near the top and bottom of the chamber is slightly colder than the bulk fuel, but near the end of the cooldown period, the vertical temperature profile becomes quite isothermal. It is apparent that the vertical temperature profiles in this system are very different from those obtained in previous Boeing [19] and Lockheed [4] simulators, in which only the top and bottom surfaces were cooled (e.g., see figure 4). It is believed that these less isothermal temperature profiles more closely represent actual aircraft fuel tank temperature profiles. To obtain more realistic temperature profiles, a heat exchanger chiller plate (figure 17) was constructed and attached to the bottom of the wing tank chamber. A Neslab ULT-95 recirculating chiller capable of operating down to

-90°C was used to circulate cooling fluid (methanol) through the chiller plate. Figure 18 shows the temperature profiles obtained during cooldown using the chiller plate. The figure shows that during cooldown, the chiller plate significantly increases cooling of the fuel near the bottom of the tank. Near the end of the cooldown period, the vertical temperature profiles become significantly more isothermal so that no benefit from the chiller plate is apparent.

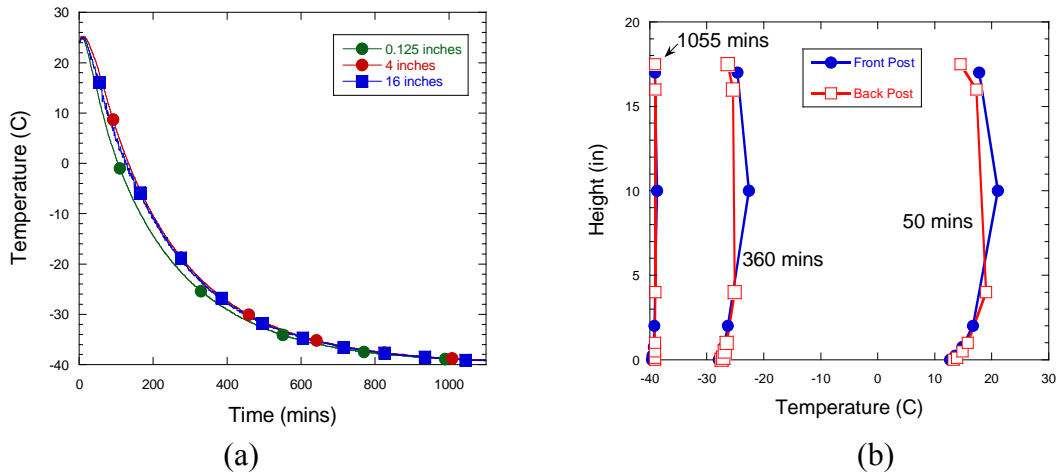


Figure 16. Temperature Profiles in the Wing Tank Simulator (a) Temperatures at Three Vertical Locations During Cooldown and (b) Vertical Temperature Profiles at Three Different Times During Cooldown

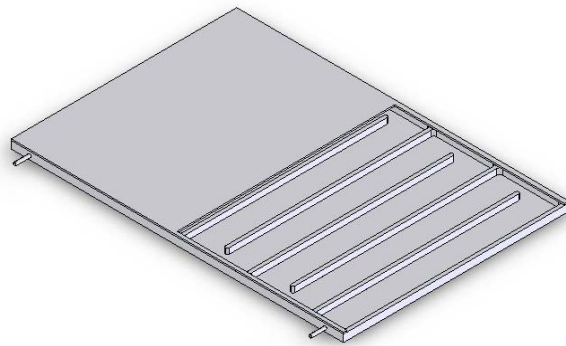


Figure 17. Design of Wing Tank Simulator Chiller Plate

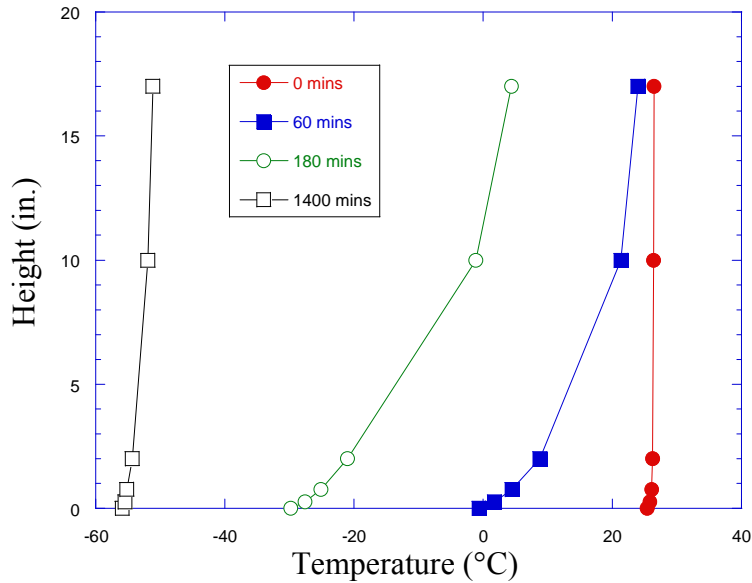


Figure 18. Height vs Temperature for Cooldown in the Wing Tank Simulator at Various Times Using the Chiller Plate

Subsequent studies using the fuel pump during recirculation and pump-out type runs indicated that the vertical temperature profile obtained was relatively unimportant to the type of studies performed for the present work. The previous Boeing and Lockheed studies explored the effect of temperature on fuel holdup, and thus required realistic vertical temperature profiles. The present work explores the flowability and pumpability of fuel as a function of temperature. Realistic fuel vertical temperature profiles are less desirable here. The relatively isothermal fuel temperatures obtained in the environmental chamber provide well-known fuel temperatures throughout the simulator tank. Thus, the experiments reported here were conducted without operation of the chiller plate.

Figure 19 shows the results from a series of fuel flowability tests performed in the wing tank simulator. These tests looked at a series of fuels (JP-8, Jet A, Jet A fuel with a low-temperature, flow-improving additive, and JPTS fuel properties shown in table 4) in which cooldown, recirculation, and pump-out runs were performed. JPTS (freeze point specification  $-53^{\circ}\text{C}$ ) and JP-8 (freeze point specification  $-47^{\circ}\text{C}$ ) fuels are refined to provide improved low-temperature capability beyond Jet A fuels. They were chosen to provide a comparison of the flowability of these improved low-temperature fuels with that of Jet A. The most informative tests were the recirculation tests, in which the fuel was cooled to a target temperature near the freeze point and subsequently pumped (via the boost pump) out the fuel inlet and back into the tank via the piccolo return tube. The pump operation results in heat being added to the fuel. This added heat resulted in a slow fuel temperature rise (approximately  $20^{\circ}\text{C}$  per hour) during recirculation. Fuel recirculation was continued until the fuel reached the target temperature of  $-37^{\circ}\text{C}$ , which is the Jet A specification maximum freeze point  $+3^{\circ}\text{C}$ . In this way, fuel recirculation was used as a method to evaluate fuel flowability and pumpability over a range of temperatures in a single experimental run. The figure shows that, for each of the fuels, as temperature increases, the flow rate increases. This observation results primarily from the decrease in viscosity with increasing

temperature, shown previously in the Brookfield viscometer measurements. For example, the flow rates were compared at the measured freeze point +3°C temperature (shown as vertical arrows for each fuel in the figure) with the flow rates at -37°C for each fuel. Flow reductions of 2.2%, 4.1%, 9.2%, and 10.2% were observed over this temperature range for fuels 3166, 3804, 4177, and 2976, respectively. This data shows that the lower freezing fuels exhibit greater flow reduction relative to the -37°C temperature than do higher freezing fuels. This important result shows that operating fuels near their measured freeze point rather than near the specification freeze point can result in reduced fuel flowability, in agreement with the viscometry measurements. The important question is how such a reduction in fuel flowability will affect aircraft and engine operation. The answer to this question is likely fuel system dependent. Each aircraft fuel system would need to be evaluated individually to evaluate the flow rate requirements of the engine. In addition, it is also important to take into account the effect of the engine's main pump on fuel flow. For example, in the Boeing 747 aircraft, the suction from engine's main pump operation may lessen the observed effect.

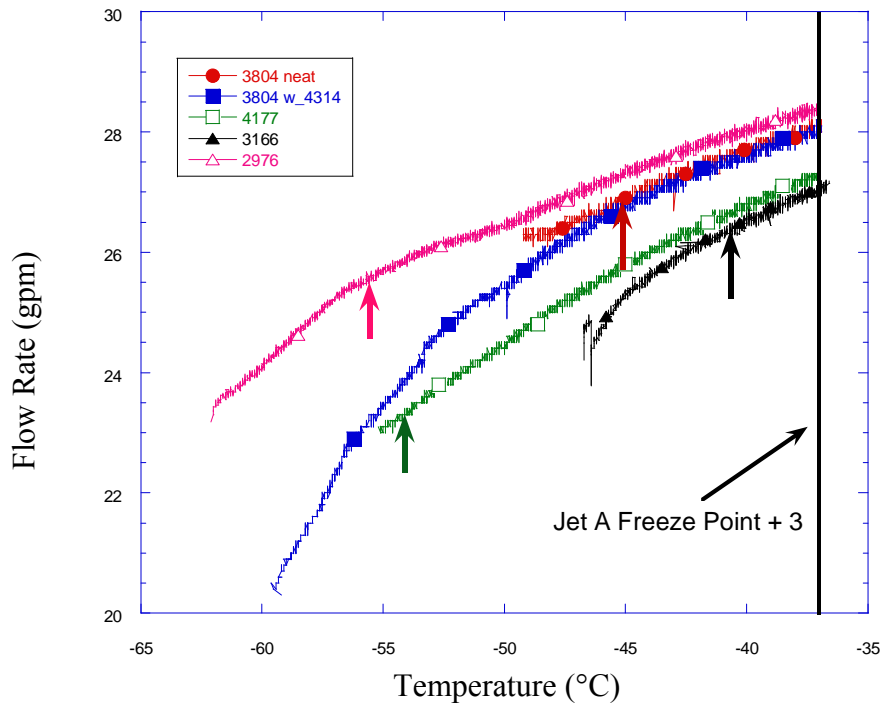


Figure 19. Flow Rate vs Temperature During Recirculation in the Wing Tank Simulator Using Five Different Fuels With the Vertical Arrows Showing the Location of the Measured Freeze Point +3°C Temperature for Each Fuel and the Vertical Black Line Showing the Jet A Specification +3°C Temperature (-37°C)

Table 4. Fuel Properties for the Wing Tank Simulator

Fuel and Type	Freeze Point (°C)	Cloud Point (°C)	Pour Point (°C)
3166 Jet A	-43.7	-46.3	-48.0
3804 JP-8	-47.6	-51.4	-56.0
4177 JP-8	-57.2	-59.1	-65.0
2976 JPTS	-58.5	-62.9	-67.5

Figure 19 also shows a comparison of the flowability of a fuel containing a candidate cold flow-improving additive (referred to here as additive 4314) with that of the unadditized fuel. The figure shows that the additized fuel remained flowable to temperatures almost 15 degrees below the fuel freeze point. In the temperature range where the two fuels overlap, their flow rates remained nearly identical. These results indicate that flow-improving additives hold promise for providing jet fuels with improved, reduced temperature capabilities [1 and 21].

#### 4. COMPUTATIONAL FLUID DYNAMIC MODELING OF FUEL TEMPERATURES IN AIRCRAFT WING TANK SIMULATORS.

As described earlier in this report, many fuel samples exhibit freeze points that are significantly lower than the specification freeze point. The use of the measured freeze point would permit lower fuel temperatures during flight, resulting in more flexibility in flight profiles. This increased flexibility can result in significant advantages for airlines and their customers, including lower ticket prices and greater flight availability. However, the influence of low temperatures on jet aircraft operations needs to be better understood. CFD permits the numerical simulation of a variety of thermal and flow conditions within a fuel tank and clarifies laboratory experiments. CFD modeling provides transient temperature and velocity profiles within a fuel tank and can demonstrate the importance of proper temperature sensor location. At temperatures near the measured freeze point, the viscosity must be low enough to permit pumping and to flow through narrow passages. In addition, it should be low enough to not degrade proper fuel atomization in combustor nozzles. Thus, it is essential to evaluate the effects of fuel temperature on viscosity and other properties. A goal of this work is to use CFD to study the low-temperature behavior of jet fuel within the current experimental fuel tank (referred to as the wing tank simulator) and in tank-cooling experiments performed elsewhere by Boeing [19] and Lockheed [4].

##### 4.1 SIMULATION METHODOLOGY.

A commercially available CFD code (CFD-ACE, CFD Research Corporation) was used to simulate the laminar, time-varying flow and heat transfer by finite volume solution of the unsteady Navier-Stokes and energy (enthalpy) equations. Equation 1 represents the momentum or energy equation depending on the variable represented by  $\Phi$  (velocity component or enthalpy). For a given  $\Phi$ ,  $\Gamma_\Phi$  is the appropriate transport coefficient, and  $S_\Phi$  is the proper source term. With respect to the momentum equation, buoyancy forces induced by temperature differences within the tank are included in  $S_\Phi$ .

$$\frac{\partial(\rho\Phi)}{\partial t} + \text{div}(\rho\vec{u}\Phi) = \text{div}(\Gamma_{\Phi} \text{grad}\Phi) + S_{\Phi} \quad (1)$$

The convective terms are represented by a third-order accurate upwind scheme, and a version of the SIMPLEC (Semi-Implicit Method for Pressure-Linked Equations Consistent) algorithm is used in the solution procedure. In studies of the effect of an ullage space on heat transfer and flow within the wing tank simulator, the volume-of-fluid (VOF) method was initially used to track the interface between the liquid fuel and air [22 and 23]. Unfortunately, the VOF method requires excessive computation time and is not practical for long-duration static cooling tests. For simplicity, only the behavior of the liquid fuel was solved and a boundary at the liquid-air interface is imposed.

Viscometer measurements provided the fuel viscosity for simulations of the current experiments, and values of the viscosity reported by the CRC [5] were used in simulations of jet fuel behavior in the Boeing [19] and Lockheed tanks [4]. In addition, values of the density, thermal conductivity, enthalpy, and specific heat for Jet A fuel were provided by the CRC and used in all simulations.

The transient boundary temperatures for only the top and bottom surfaces were reported in the Boeing and Lockheed studies. Thus, only two-dimensional simulations were performed for the Boeing and Lockheed conditions. It was assumed that the largest changes in temperature would occur in the direction normal to the top and bottom surfaces, and that the other surfaces of the tanks were insulated. For relatively thin, long wings, this is a reasonable thermal boundary condition for regions away from the wing tips. Because a rack of thermocouples was located near the center of the Boeing and Lockheed tanks, it was reasonable to assume that the behavior there would be approximately two-dimensional and could still be compared with two-dimensional temperature solutions. Thus for simplicity, CFD calculations were performed using two-dimensional unstructured grids generated from the geometries of the Boeing and Lockheed tanks (figure 20(a) and (b)). In the Boeing tank case (figure 20(a)), two Z-stringers were attached to the bottom surface of the tank. With regard to the Lockheed tank geometry, three Z-stringers were attached to the upper surface, while three I-stringers were attached to the bottom surface. In the current Federal Aviation Administration (FAA) experiments, the transient temperature profiles of all the walls are known. Thus, both two- and three-dimensional grids representing the FAA simulator were employed. The actual aluminum tank has a baffle rib in the center with three check valves (4.7 cm diameter). As figure 20(c) shows, the three-dimensional geometry of the simulations involves two compartments, which have three circular passages available for flow. In the simulations, the check valves are represented by holes for simplicity, as they offer little flow resistance. Also, two Z-section stringers (7.6 cm high) located at the bottom of the tank are represented in the calculations. The internal dimensions of the Boeing and Lockheed tanks [19 and 4] are similar to those of the wing tank simulator.

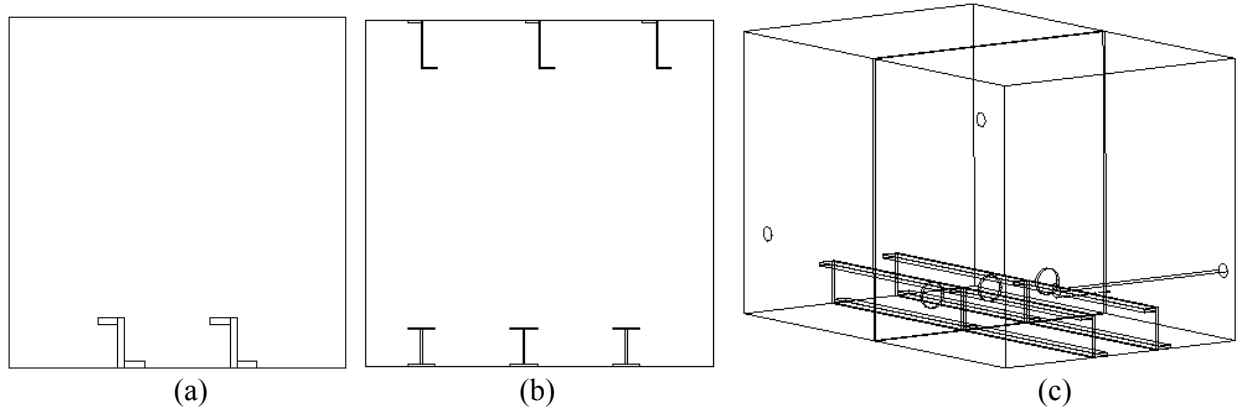


Figure 20. Two-Dimensional Geometries Representing (a) the Boeing Tank, (b) the Lockheed Tank, and (c) the Three-Dimensional Geometry of the Wing Tank Simulator

In the experiments performed using the wing tank simulator, the emphasis was on static cooling. Thus, in most simulations of the wing tank simulator, the flow was not pumped, but rather, was driven by buoyancy forces resulting from the transient cooling of the fuel tanks. The temperature boundary conditions for the wing tank simulator wall came from a spatial average of the thermocouples imbedded in a wall. These spatial averages were obtained as a function of time and were then used as the transient temperature boundary condition in the calculations. The initial fuel temperature was assumed to be uniform.

Table 5 lists the more important simulations that were performed in this study. It is important to study the influence of tank geometry and fuel properties on heat transfer. Fuel temperature measurements resulting from different tank geometries and imposed cooling regimens are compared with simulations for code validation. Simulations 1 and 2 correspond to previously performed Lockheed and Boeing experiments while Simulations 3 through 11 are for the FAA tank to simulate static cooling. For the Lockheed test (Simulation 1), the top and bottom walls have uniform temperatures varying in time, while the sidewalls are assumed to be adiabatic as temperatures there are not available. The Boeing test (Simulation 2) is assumed to have isothermal horizontal surfaces and adiabatic vertical walls. Simulations 5 through 7 were performed to study the behavior of the fuel temperature profile when properties (density and viscosity) are artificially varied. The objective of Simulation 6 was to study the effect of two different jet fuel viscosities on the fuel flow and temperature. In Simulation 3, the vertical walls were assumed to be adiabatic. The reason for using adiabatic boundary conditions was to study how the flow and temperature distribution are affected by an adiabatic boundary relative to walls of uniform temperature. In all the other FAA simulations (Simulation 4 through 12), the temperature of the sidewalls along with the top and bottom walls decreased uniformly in time. In the simulations, it was assumed that the tank is full except for Simulations 8 and 11. In Simulation 8, an air gap of either 3.8 or 26.5 cm was included, and in Simulation 11, an air gap of 3.8 cm was used. Two-dimensional grids were used in Simulations 1 through 9 and three-dimensional grids were used in Simulations 10 through 12. To understand how the fuel flowing into the tank would affect the thermal profile of the tank, an unstructured grid with a piccolo tube (to allow the return flow) was simulated, as indicated in Simulation 12 for the wing tank simulator.

Table 5. Select CFD Simulations

Simulation No.	Experiment	Grid	Objective	Boundary Conditions
1	Lockheed Test 140	2D Unstructured	Simulate previous static-cooling experiment	Top and bottom walls—uniform, transient temperature side walls—adiabatic
2	Boeing Test 439/505	2D Unstructured	Simulate previous static-cooling experiment	Top and bottom walls— isothermal at 221.9 K side walls—adiabatic
3	FAA Test 30	2D Unstructured	Simulate static-cooling experiment (figures 27-29)	Top and bottom walls— uniform, transient temperature side walls—adiabatic
4	FAA Test 30	2D Unstructured	Simulate static-cooling Experiment	Top and bottom walls— uniform, transient temperature side walls—uniform, transient temperature
5	FAA No experimental data	2D Unstructured	Increase in viscosity by 200% and 30%	Top and bottom walls— uniform, transient temperature side walls—uniform, transient temperature
6	FAA No experimental data	3D Structured	Comparison of viscosity of fuels—3219 and 3633	Top and bottom walls— uniform, transient temperature Side walls—uniform, transient temperature
7	FAA No experimental data	2D Unstructured	Density change by 5%	Top and bottom walls—uniform, transient temperature side walls— uniform, transient temperature
8	FAA Test 42	2D Structured	Simulate static-cooling experiment with ullage space	Top and bottom walls—uniform, transient temperature side walls— uniform, transient temperature
9	FAA Test 42	2D Unstructured	Simulate static-cooling experiment	Top and bottom walls—uniform, transient temperature side walls— uniform, transient temperature
10	FAA Test 42	3D Unstructured	Simulate static-cooling experiment	Top and bottom walls—uniform, transient temperature side walls— uniform, transient temperature
11	FAA Test 42	3D Structured	Simulate static-cooling experiment with ullage volume	Top and bottom walls—uniform, transient temperature side walls— uniform, transient temperature

2D = two dimensional  
3D = three dimensional

When the global error residuals were reduced below four orders of magnitude from their maximum values, the solution was considered to be converged. Table 6 shows studies for the three different types of grids used for the transient calculations. It includes an unstructured grid

for the two-dimensional calculations and structured grids for three-dimensional simulations. A course grid was refined by increasing the number of cells until grid independence was achieved. The two-dimensional unstructured grid, initially made with 1672 cells, was refined by increasing the number of cells to as much as 6065. Results using the grid with 3057 cells are presented in table 6. The table shows the calculated bulk fuel temperature at different locations for different grid sizes. There is negligible change in the temperature of the bulk fuel with variation in the grid cells. Similarly, a three-dimensional structured grid representing the wing tank simulator, with and without ullage space, was studied for grid independence of the solution. The number of cells used for the full tank was increased from 21,866 to 87,438. Results from the grid with 52,234 cells are described in this work. Further grid refinement resulted in negligible changes in the solutions.

Table 6. Grid Studies for Different Conditions (All temperatures are in degrees Kelvin. Number of cells in bold represent the grids used for the calculations described in the results.)

Two-Dimensional Unstructured Grid				
Location		9 cm From Top	1 cm From Side	1 cm Above Bottom
No.	Cells	Temperature	Temperature	Temperature
1	1,672	231.2	225.1	219
<b>2</b>	<b>3,057</b>	<b>229</b>	<b>224.8</b>	<b>219.8</b>
3	6,065	229.6	225.2	218.5
Three-Dimensional Structured Grid (Full Tank)				
Location		Tank Center	1 cm From Top	1 cm Above Bottom
No.	Cells	Temperature	Temperature	Temperature
1	21,866	271.3	236.8	233.9
2	32,760	271	236.3	234.3
<b>3</b>	<b>52,234</b>	<b>270</b>	<b>234.7</b>	<b>233.6</b>
4	87,438	270.7	234.2	232.8
Three-Dimensional Structured Grid (Ullage case)				
Location		Tank Center	6 cm From Top	1 cm Above Bottom
No.	Cells	Temperature	Temperature	Temperature
<b>1</b>	<b>50,715</b>	<b>293.8</b>	<b>293.7</b>	<b>285.3</b>
2	144,000	293.8	293.7	286

## 4.2 SIMULATIONS OF BOEING AND LOCKHEED STATIC-COOLING EXPERIMENTS.

### 4.2.1 Lockheed Tank Simulations.

To better understand the implication of the location of fuel tank temperature sensors and the resulting relationship to the measured freeze point temperature, it is important to simulate how

the temperature of the fuel varies within a cooled fuel tank. Here, previously performed Lockheed low-temperature experiments that represent the cooling of a portion of a commercial fuel tank (Simulation 1, table 5) have been numerically simulated. The time-dependent simulations use a two-dimensional unstructured grid and represent the flow near the center of the chamber. The sidewalls are considered to be adiabatic, while the top and the bottom skin temperatures vary with time following the prescribed schedule of the Lockheed experiments (Test 140, [4]). The skin temperatures decrease from 22°C initially to -32°C. The fuel temperature is initially at 22°C but decreases to a minimum of -30°C (near the wall) at the end of the experiment.

Figure 21(a) and (b) show the color contour plots of the temperature profile observed in the Lockheed tank after 6 and 7 hours, respectively. Much of the heat conduction is through the stringers. The dense, cold fuel settles at the bottom of the tank. After 6 hours of cooling, most of the fuel in the tank is at 280 K. After 7 hours, the bulk fuel is at 275 K. Figure 22 shows measured and calculated temperature profiles of these two cases. The measurements are from five thermocouples located at different heights from the bottom surface on a rack near the center of the tank. Figure 22 shows that there is fair agreement between the measurements and calculations near the lower wall (up to 5 cm above the lower surface) for both cooling periods. However, further above the bottom of the tank, there are larger differences between the measured and calculated temperatures. Also, near the top surface, there is a sudden change in temperature due to the presence of stringers attached to the top surface. In addition, figure 22 shows that these larger temperature differences decrease with the longer cooling period of 7 hours. Given the uncertainty in the temperature conditions of the vertical surfaces in the simulations (assumed adiabatic), such differences between measured and simulated temperatures away from the lower surface were expected.

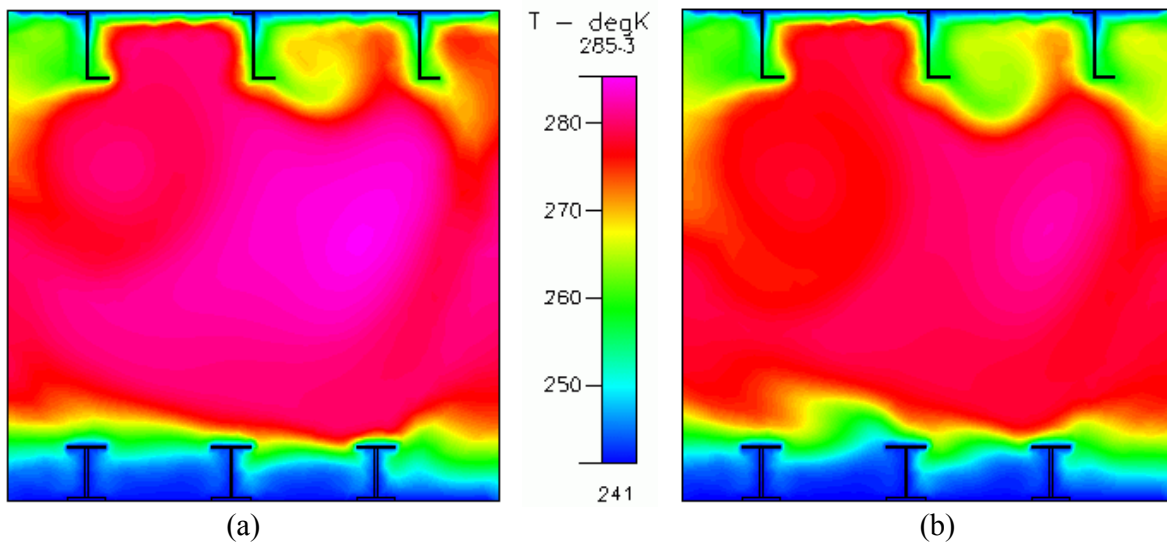


Figure 21. Color Contour Plots Showing Simulated Temperature Profiles in the Lockheed Tank After (a) 6 Hours and (b) 7 Hours of Simulation

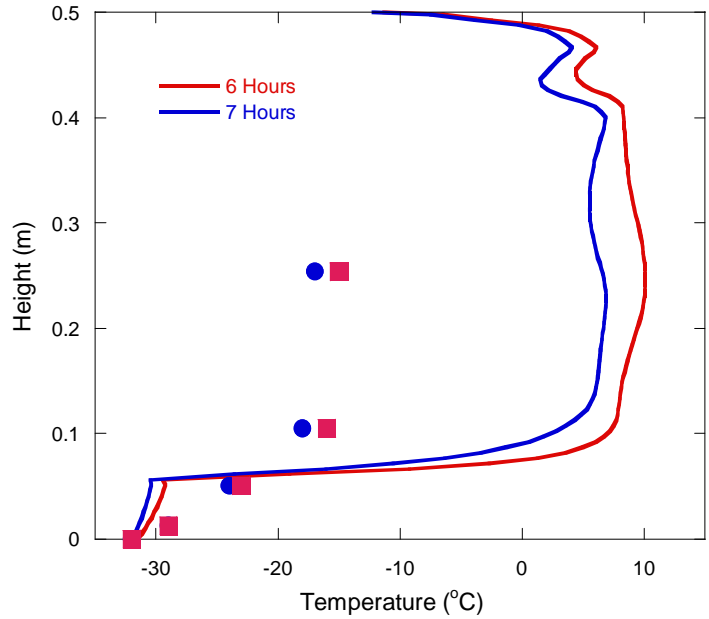


Figure 22. Measured and Calculated Temperature Profile Above the Tank Bottom Near the Tank Center for 6- and 7-Hour Cooling Periods for the Lockheed Experiment, With the Symbols Representing Measured Temperatures

Figure 23 shows measured and predicted temperatures for a thermocouple located 1.3 cm from the tank bottom and near the tank center over a 6-hour period. Note that the temperature decreases with time but ultimately levels at this location. The measured and simulated temperatures agree well as they are near the lower surface boundary where there is less influence from the vertical surfaces.

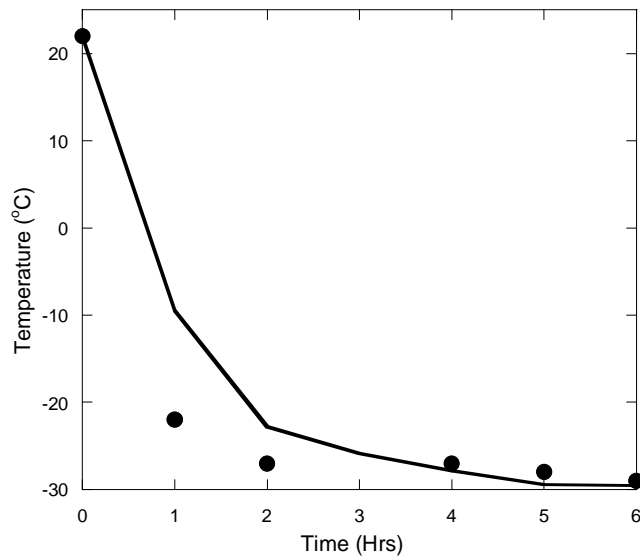


Figure 23. Measured and Simulated Time-Varying Fuel Temperature 1.3 cm Above Lower Tank Surface in the Lockheed Tank, With the Symbols Representing Measured Temperatures

#### 4.2.2 Boeing Tank Simulations.

In time-dependent simulations of the Boeing experiments (Test 439, [19]), the flow was buoyancy-driven. A two-dimensional, unstructured grid was assumed to represent the flow near the center of the chamber that did not contain the piccolo tube (Simulation 2, table 5). The temperature of the top and bottom surfaces are 221.9 K (-51.1°C), while the fuel is initially at 294 K (21°C). Figure 24(a) and (b) are color contour plots of the temperature after 1 and 15 minutes of cooling, respectively. After 1 minute of cooling, figure 24(a) shows that heat conduction through the stringers enhances cooling of the fuel. After 15 minutes, figure 24(b) shows more temperature stratification around the stringers and the start of cold fuel flowing from the upper surface. Figure 24(a) and (b) show that the temperature gradient is largest near the cooled upper and lower surfaces. Figure 25 shows that there is a large temperature gradient near the lower cooled surface, as also shown in figure 24. As in the case of the Lockheed fuel tank, the vertical surfaces were assumed to be insulated, as the temperature conditions were not available. Thus, as observed for the Lockheed tank geometry, agreement with the measured and simulated temperatures near the tank bottom is better than near the tank center.

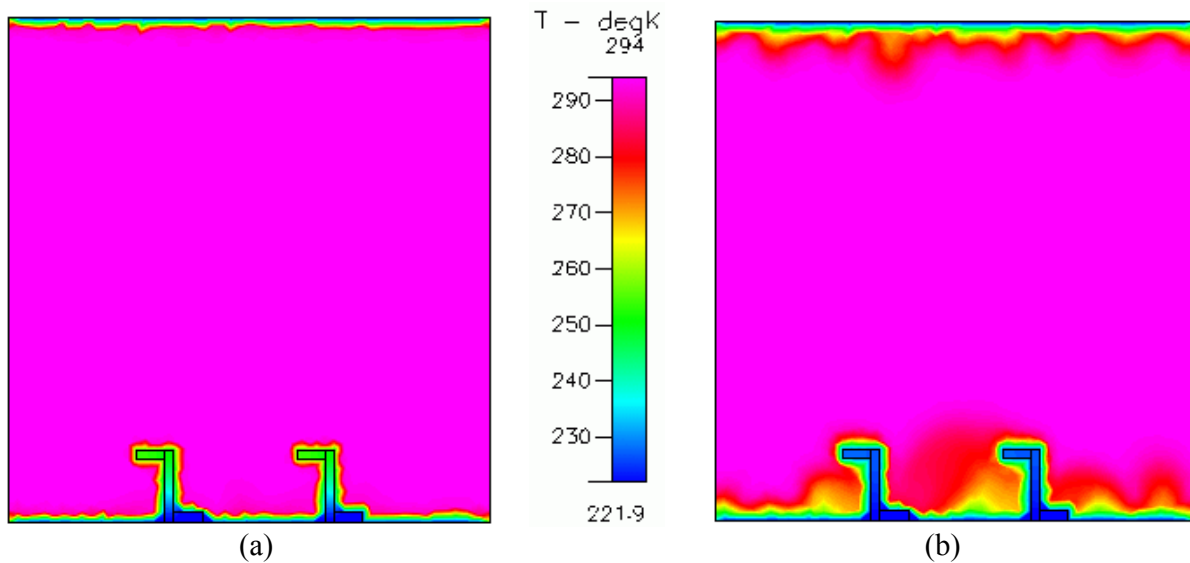


Figure 24. Two-Dimensional, Transient Simulations of Cooling of the Boeing Tank After (a) 1 and (b) 15 Minutes With Identical Upper and Lower Surface Temperatures and Buoyancy-Driven Flow

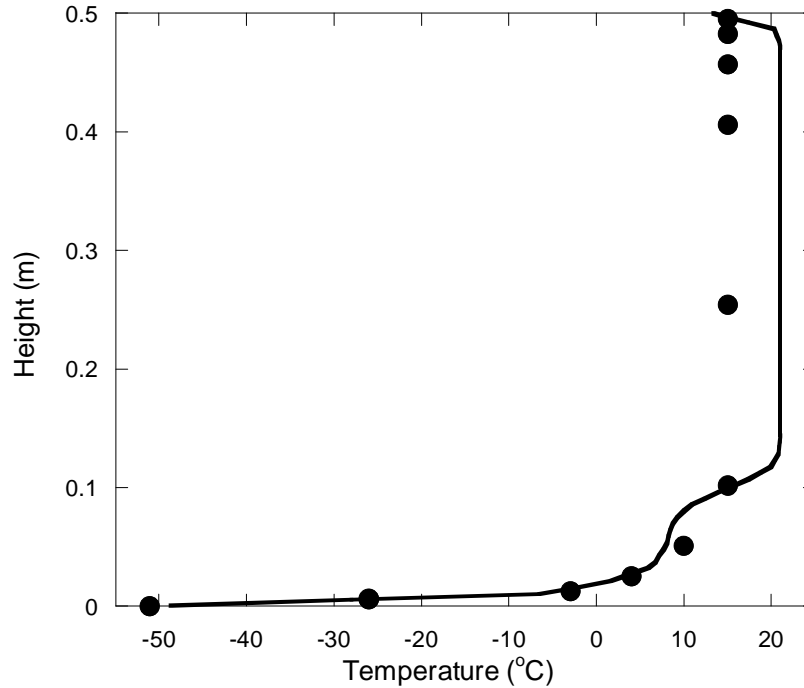


Figure 25. Measured and Simulated Fuel Temperature Distribution After 15 Minutes Above the Cooled Bottom Surface for Experiments Conducted by Boeing

### 4.3 SIMULATIONS OF FUEL COOLING WITHIN THE WING TANK SIMULATOR.

Two-dimensional simulations require much less computer memory and fewer computations than the three-dimensional simulations of the experimental vessels. However, the two-dimensional simulations may offer less fidelity with respect to velocity and temperature than the three-dimensional solutions. To study if three-dimensional calculations can be reasonably replaced by two-dimensional calculations for simplicity, both two- and three-dimensional calculations were performed.

#### 4.3.1 Two-Dimensional Simulations.

Simulations were performed to study the differences in the calculated temperature profiles within the wing tank simulator for conditions of adiabatic vertical walls or vertical walls in which the temperature uniformly decreased (Simulations 3 and 4, table 5). As shown in figure 26, for the calculations, the fuel was initially at 295 K, and the top and bottom walls were uniform in temperature, changing with time from 293.5 K initially to 217.7 K after 15 hours. The vertical walls were either insulated or uniform with an initial temperature of 294.5 K, which decreased to 219.7 K. Figure 27(a) and (b) show that near the tank center, the fuel is relatively warm and that cooler fuel tends to reside near the stringers on the tank bottom. However, as indicated by the fuel temperature contours, the flow is very different for the two sets of imposed wall conditions. In figure 27(a), as the vertical walls are also cooled with the horizontal walls, a thermal boundary layer can be observed adjacent to the vertical walls. In figure 27(b), the adiabatic sidewalls result in uneven fuel motion and temperature distribution. As might be expected, figure 27

shows that, overall, the fuel is cooler when the sidewalls are also cooled with the horizontal surfaces.

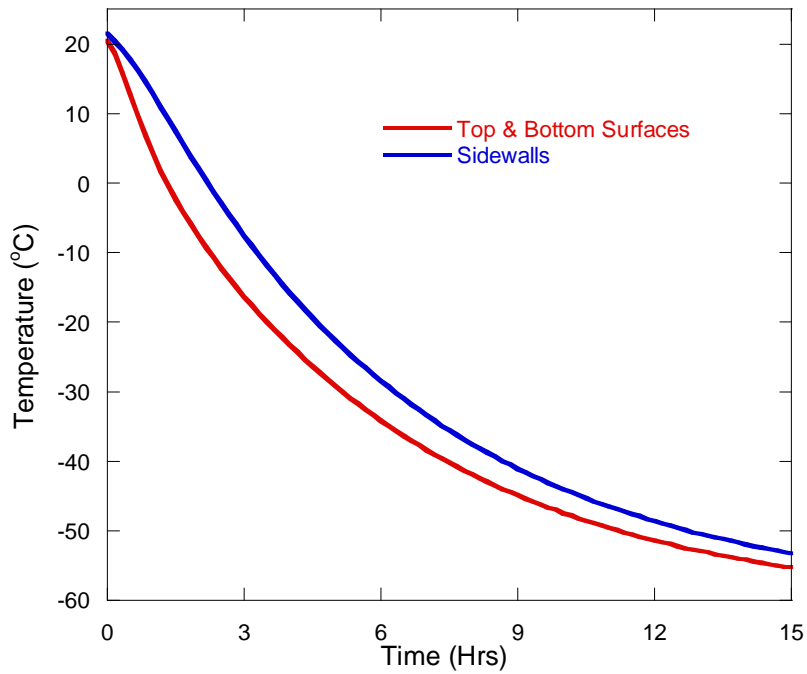


Figure 26. Skin Temperature Schedule for FAA Test 30

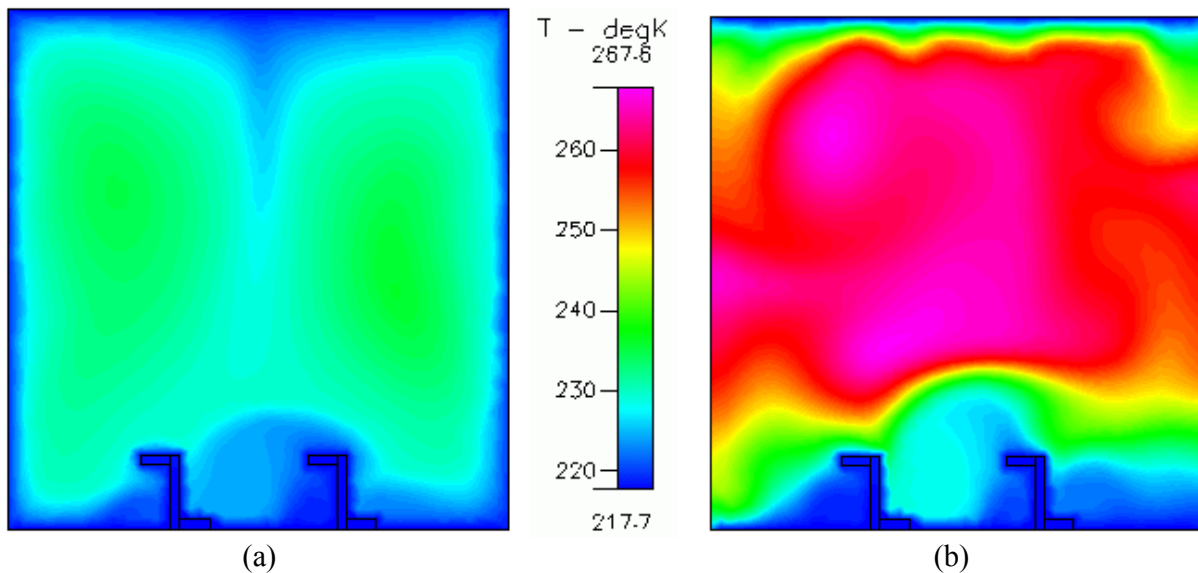


Figure 27. Two-Dimensional Simulations of Cooling in the Wing Tank Simulator After 15 Hours for (a) Vertical Walls of Uniform Temperature and (b) Insulated Vertical Walls

Figure 28(a) and (b) show the vector plots describing the fuel flow behavior in the tank for these two different vertical wall conditions. In figure 28(a), there are two nearly symmetrical vortices. On the other hand, the flow shown in figure 28(b) is more complex with several smaller vortical

cells. Figure 29(a) and (b) show the thermal profiles for the two vertical wall boundary conditions at two different thermocouple locations. There is a large temperature difference for the thermocouple located at about 1.2 cm from the sidewall, as shown in figure 29(a). The sidewalls with uniform temperature profile are in better agreement with the measured values relative to the adiabatic sidewalls. In figure 29(b), for the thermocouple located 1.3 cm from the bottom wall, the measured and calculated temperatures are in good agreement for both vertical wall cases, as they are near the lower surface boundary where there is less influence from the vertical surfaces. Thus, the choice of transient uniform temperature or heat flux boundary conditions imposed on a computational grid has a large influence on the resulting computations. An important advantage of using the newly fabricated wing tank simulator is that it provides numerous thermocouple readings about all tank surfaces. Thus, the necessity of assuming boundary conditions for the vertical surfaces for purposes of comparison with experimental measurements, as in the two-dimensional numerical simulations of the Boeing and Lockheed experiments, is eliminated using the wing tank simulator.

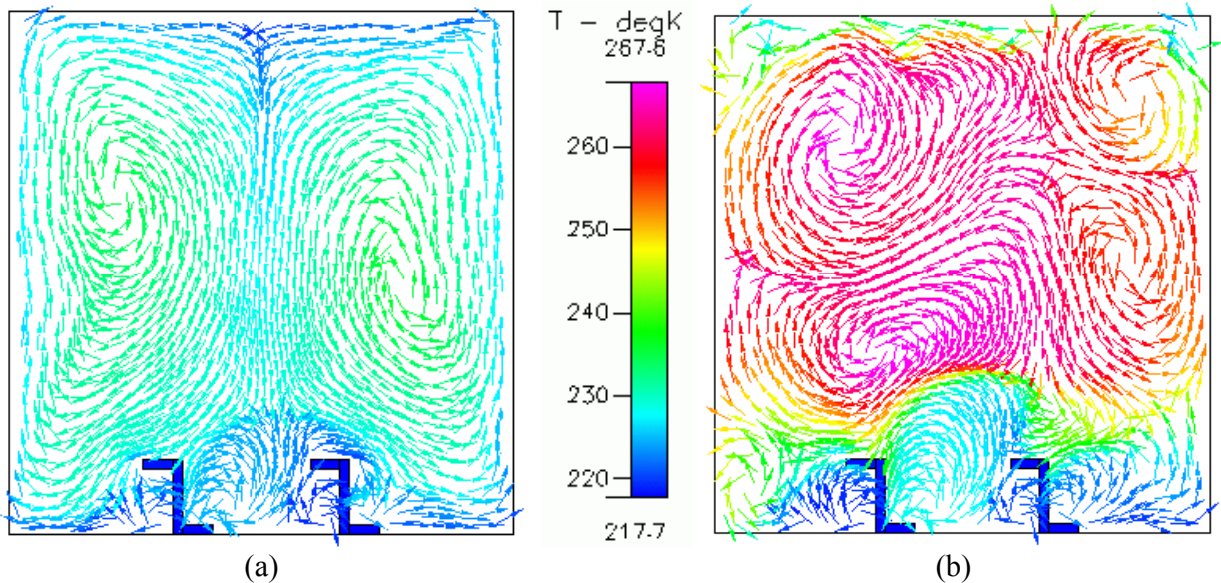


Figure 28. Vector Plots Showing Flow in the Wing Tank Simulator After 15 Hours for (a) Vertical Walls of Uniform Temperature and (b) Insulated Vertical Walls

Two-dimensional simulations of the wing tank simulator were used to study the effects of viscosity, density, and ullage space on the resulting temperature and velocity profiles within the fuel. It is known that fuel samples that meet a particular fuel specification but originate from different refineries may have different viscosities and densities at the same temperature. Thus, it is important to simulate how a variation in a particular fuel property can influence the flow and temperature within a cooled fuel tank. For simulations of property variations using the wing tank simulator, the tank was assumed to be filled with liquid fuel. A two-dimensional grid, which represents the flow near the center of the chamber, was employed in the calculations.

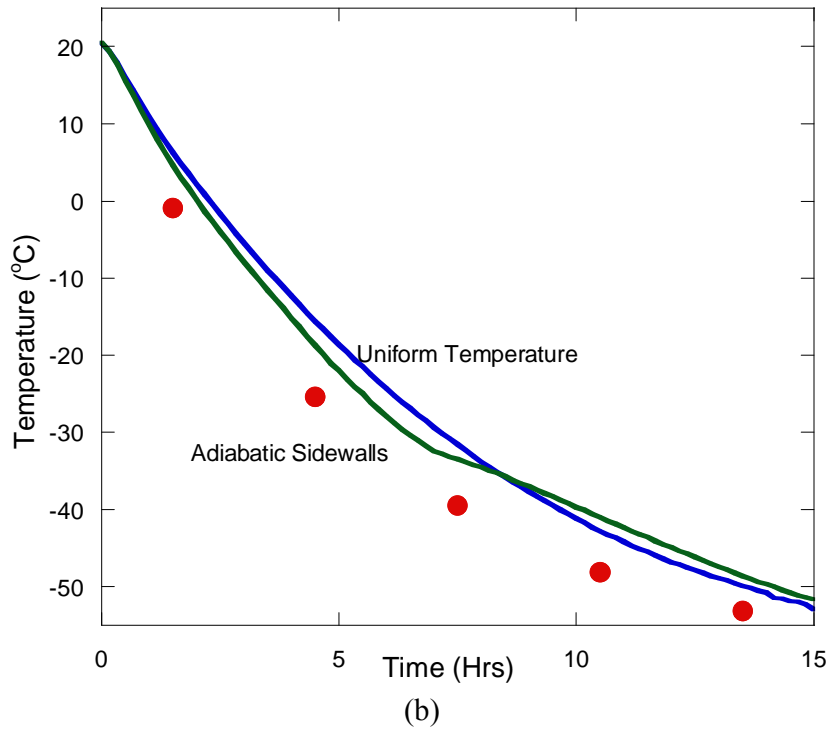
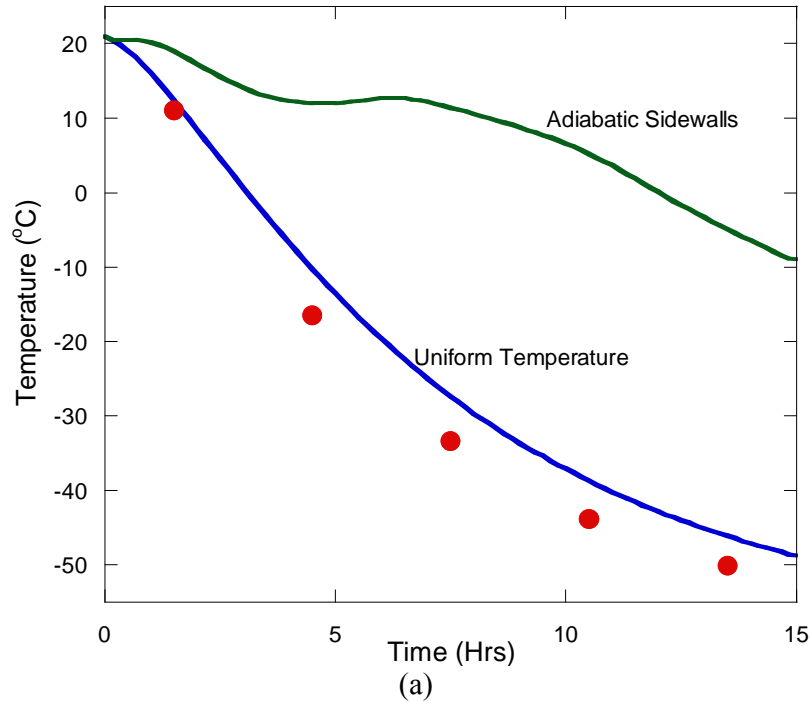


Figure 29. Measured and Simulated Temperatures for Uniform Wall Temperature or Adiabatic Boundary Conditions for Thermocouples Located (a) 1.2 cm From the Sidewall or (b) 1.3 cm Above the Bottom Wall, With the Symbols Representing Measured Temperatures

CFD calculations were used to understand the effect of changes in viscosity of the fuel using the temperature profile produced in the simulator tank (Simulations 5 and 6, table 5). The boundary conditions followed the skin temperature schedule of figure 30. The fuel was initially at 294 K and the temperature of the horizontal and vertical walls decreased uniformly after 4 hours to 222.7 K and 240.3 K, respectively. For the calculations, the viscosity of the baseline fuel was increased by either 30% or 200%, as shown in figure 31. These relatively large changes in viscosity were studied because large changes in the viscosity may occur for real jet fuels upon cooling, as shown earlier in figure 5. Figure 32(a) through (c) show the results obtained after 4 hours of cooling. All simulations showed cooler fuel residing near the stringers and two vortical cells. Less convective motion and reduction in temperature was observed when the viscosity was increased. The contour plots show that the average temperature along the horizontal line at the center of the tank was nearly 270.9 K for the baseline fluid viscosity. The temperature increases to 272.6 K and 278.0 K for 30% and 200% increase in viscosity, respectively. Therefore, it is evident that a 30% change in viscosity has little effect on the bulk fuel and does not change the temperature profile by more than 2 K. With a change in viscosity of 200%, the overall temperature of the bulk fuel in the tank changes by as much as 7 K. Three-dimensional calculations were also performed to understand the effect of change in viscosity on the temperature profile in the simulator tank using the measured temperature-dependent viscosities of two Jet A fuel samples. As previously shown in figure 6, viscosities of nine different jet fuel samples were measured at temperatures below  $-40^{\circ}\text{C}$ . Among these samples, fuels 3219 and 3633 exhibited a maximum viscosity difference (10 to 15 cP) between each other. Therefore, viscosities of these two samples were used in the calculations. Figure 33 shows a plot of height versus temperature after 4 hours. The identical profiles of the results from these two fuels indicate that a viscosity difference of 10 to 20 cP does not significantly affect the temperature profile in the tank.

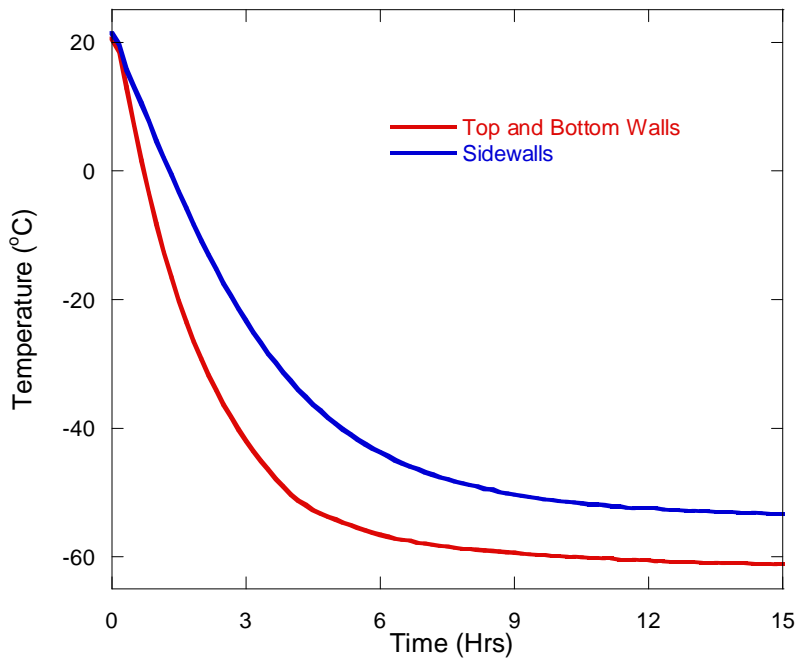


Figure 30. Skin Temperature Schedule for FAA Test 42

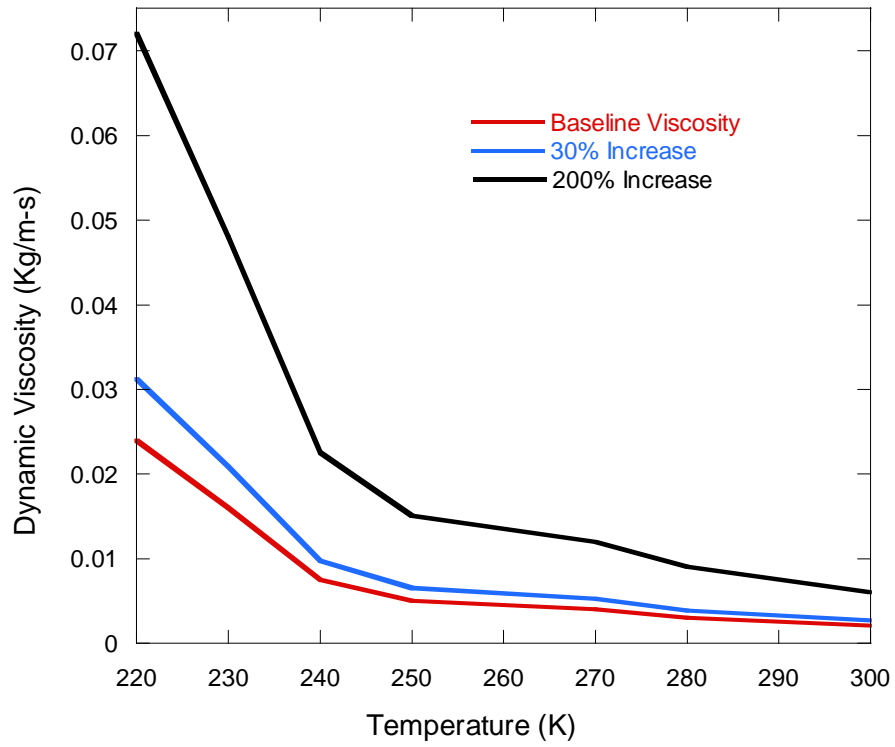
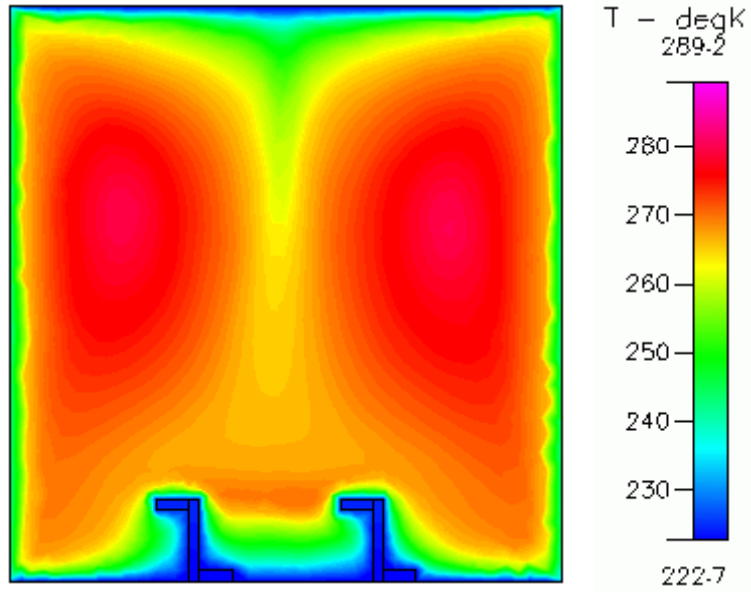
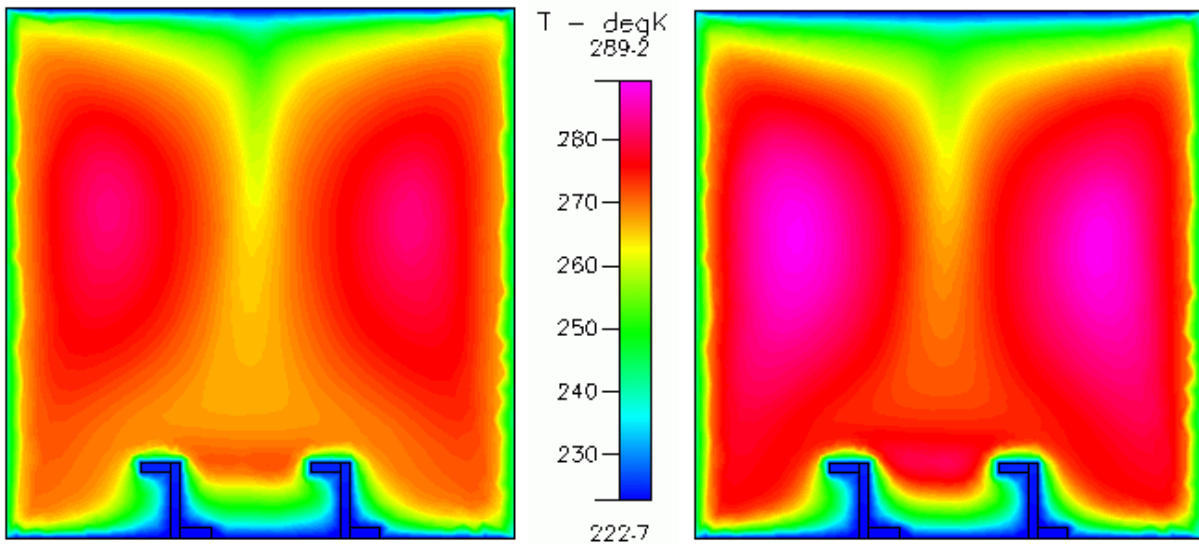


Figure 31. Dynamic Viscosity vs Temperature for Increases in Viscosity by Either 30% or 200% Relative to the Baseline Viscosity



(a)



(b)

(c)

Figure 32. Two-Dimensional, Time-Varying Simulations of the Fuel Temperature After 4 Hours of Cooling for (a) the Baseline Fuel Viscosity, (b) an Increase in Viscosity by 30%, and (c) an Increase in Viscosity by 200%

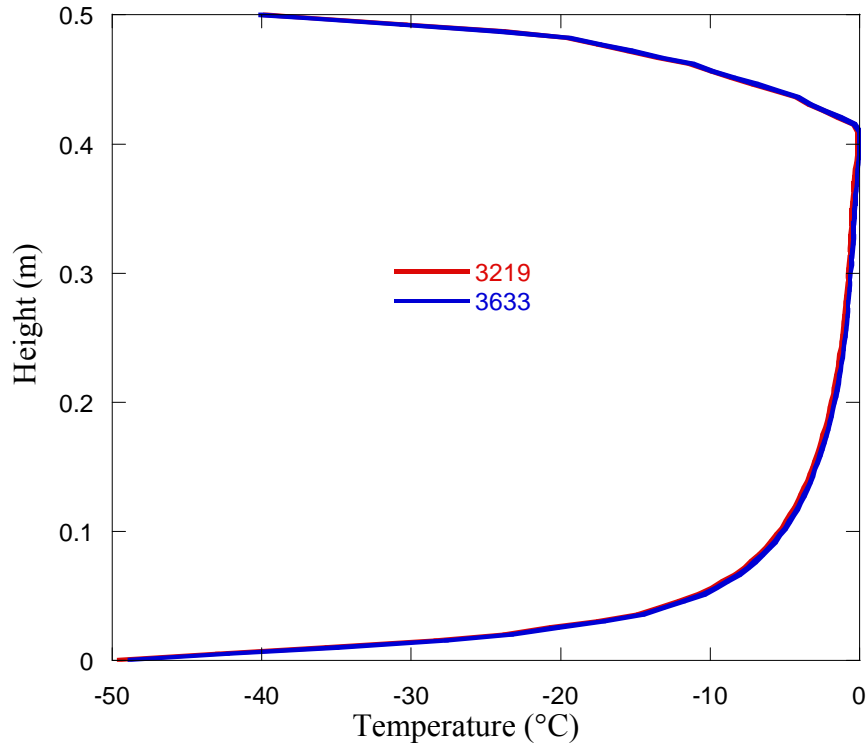


Figure 33. Vertical Temperature Profile Near the Center of a Tank Compartment After 4 Hours of Cooling for Two Different Jet Fuels

It was interesting to study how variations in fuel density change the resulting temperature distribution in the wing tank simulator, given otherwise identical conditions (Simulation 7, table 5). According to specifications (ASTM D 4052), the density of jet fuel can vary by not more than  $\pm 5\%$  ( $775 \text{ Kg/m}^3$  to  $840 \text{ Kg/m}^3$ ) at  $15^\circ\text{C}$ . In performing two-dimensional CFD simulations, the density was varied by  $\pm 5\%$  from the baseline fuel density, as shown in figure 34. The skin temperature follows the schedule of figure 30. The temperature contours (not shown here) were nearly identical in both cases with the lower-density fuel having a slightly lower-average bulk temperature of  $258.1 \text{ K}$ , as compared to  $259.4 \text{ K}$  for the higher-density fuel (calculated along the tank vertical centerline). It is not surprising that these relatively small changes in density resulted in little change in the simulated tank temperatures. Figure 35 shows a plot of temperature as a function of distance above the lower surface after 4 hours of cooling at the center of the tank. The temperature profile is similar for all three cases with small differences in temperature (about  $1^\circ$  to  $2^\circ\text{C}$ ) near the center of the tank.

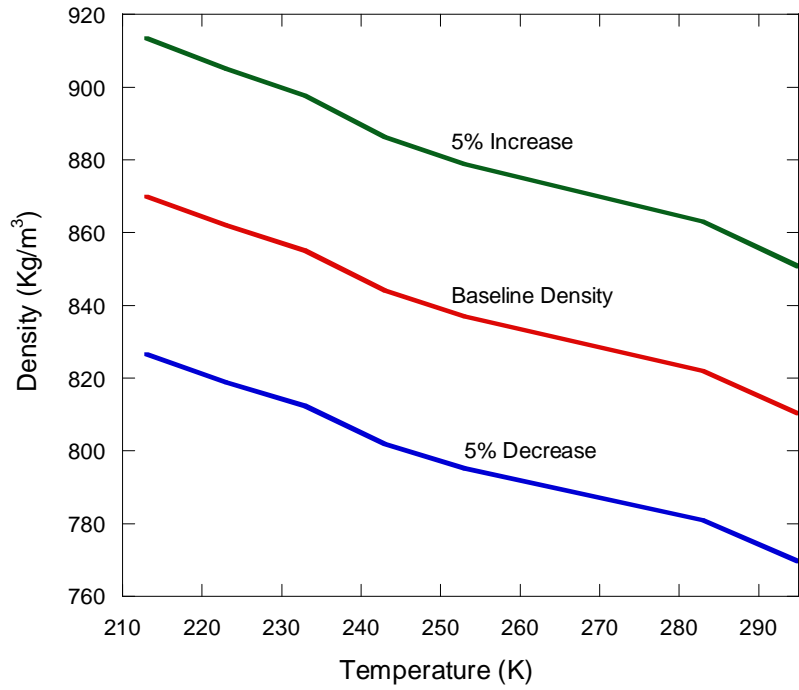


Figure 34. Density vs Temperature for Changes in Density by  $\pm 5\%$  From the Baseline Density

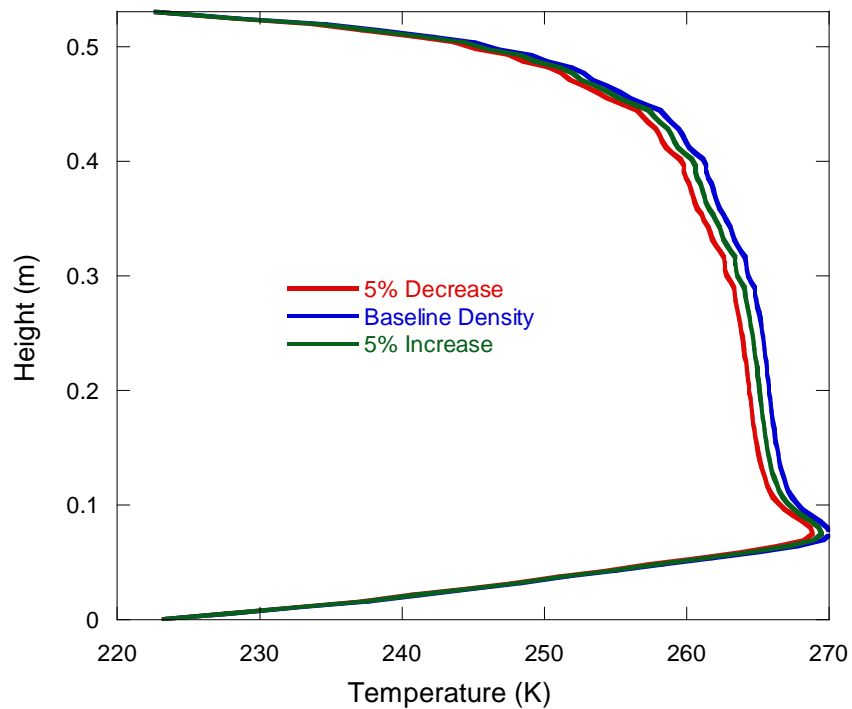


Figure 35. Transient Temperature Profile Above Lower Surface at the Vertical Centerline After 60 Minutes of Cooling for a Change of  $\pm 5\%$  From the Baseline Density

In much of the current work, the heat transfer and flow was simulated for conditions in which a tank is entirely filled with fuel. However, an aircraft fuel tank generally has an ullage space above the fuel. Thus, the effect of the ullage space (3.8 or 26.5 cm in height) on the fuel temperature (Simulation 8, table 5) was considered. These simulations follow the skin temperature schedule of figure 30. The top and bottom walls are uniform in temperature, which are initially at 293.6 K and decrease to 222.7 K after 4 hours. The sidewalls are also uniform in temperature and are cooled from 294.4 K to 240.3 K.

As described earlier, the VOF method is impractical for long-duration simulations. Hence, the calculations were simplified by assuming an adiabatic fuel-air interface. It is reasonable to assume an adiabatic condition at the fuel-air interface as the convective heat transfer coefficient on the air side of the interface is small ( $\sim 1 \text{ W/m}^2\text{K}$ ) for natural convection. In addition, since primary interest is in the bulk behavior of the media, surface tension was neglected. Hence, the fuel-air interface was assumed to be planar. The viscosity of the air is orders of magnitude smaller than that of the fuel. Thus, it was assumed that the shear stresses on the fuel at the interface were insignificant. Figure 36 shows calculated temperature contours representing 4 hours of cooling.

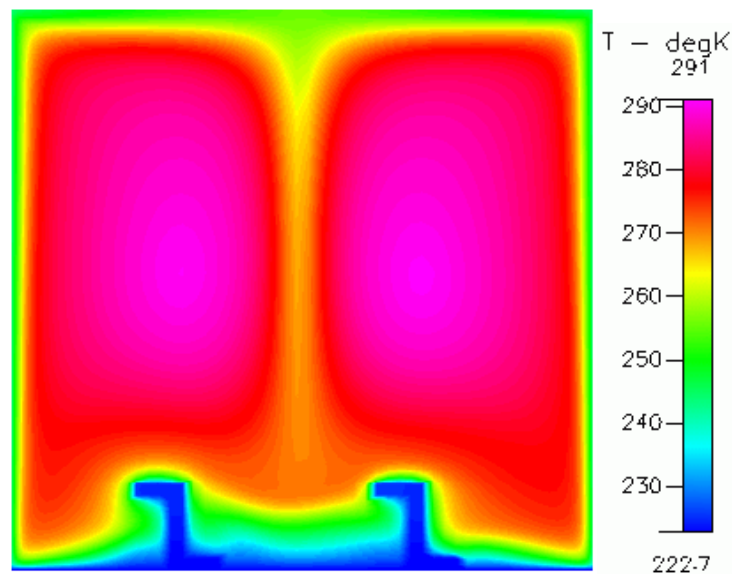


Figure 36. Two-Dimensional Thermal Profile With Adiabatic Top Surface to Represent Ullage Space (Height 3.8 cm) After 4 Hours of Cooling

Figure 37 shows the results of numerical simulations of the wing tank simulator, with and without an ullage space. The plot shows height versus temperature at a central horizontal location in the tank after 4 hours of cooling. The figure shows that the overall temperature in the tank is about  $5^\circ\text{C}$  lower when the tank is full, relative to the tank that has an ullage space. This occurs due to the heat transfer from both the top and bottom surfaces. In contrast, with the ullage space, the air gap limits the heat transfer with the top surface and results in higher temperatures in the tank.

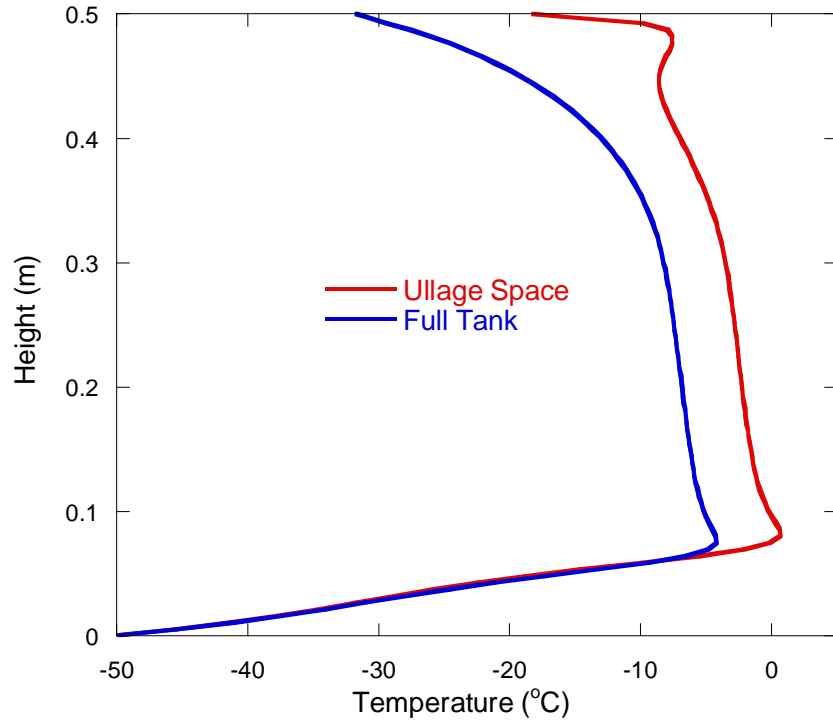


Figure 37. Effect of the Ullage Space on the Fuel Temperature Profile Along the Vertical Centerline After 4 Hours of Cooling

Figure 38(a) shows the temperature contours when the tank is full. Figure 38(b) and (c) show the results of the simulations performed with an air gap of either 3.8 or 26.5 cm at the top of the wing tank simulator after 40 minutes. The volume occupied by air for these two ullage spaces should be  $0.015 \text{ m}^3$  and  $0.1 \text{ m}^3$ , respectively. These simulations also follow the skin temperature schedule of figure 30 (Test 42). It is evident from the plots that the air gap insulates the fuel from the upper tank surface and much of the fuel near the center of the tank remains at a relatively warm temperature. Figure 39 compares measured (Test 42) and simulated (two-dimensional) transient temperatures at one location in the fuel (center of a tank compartment). Differences between the measurements and the simulations are believed to be due to three-dimensional effects, such as cooling of the fuel by the center wall in the actual tank.

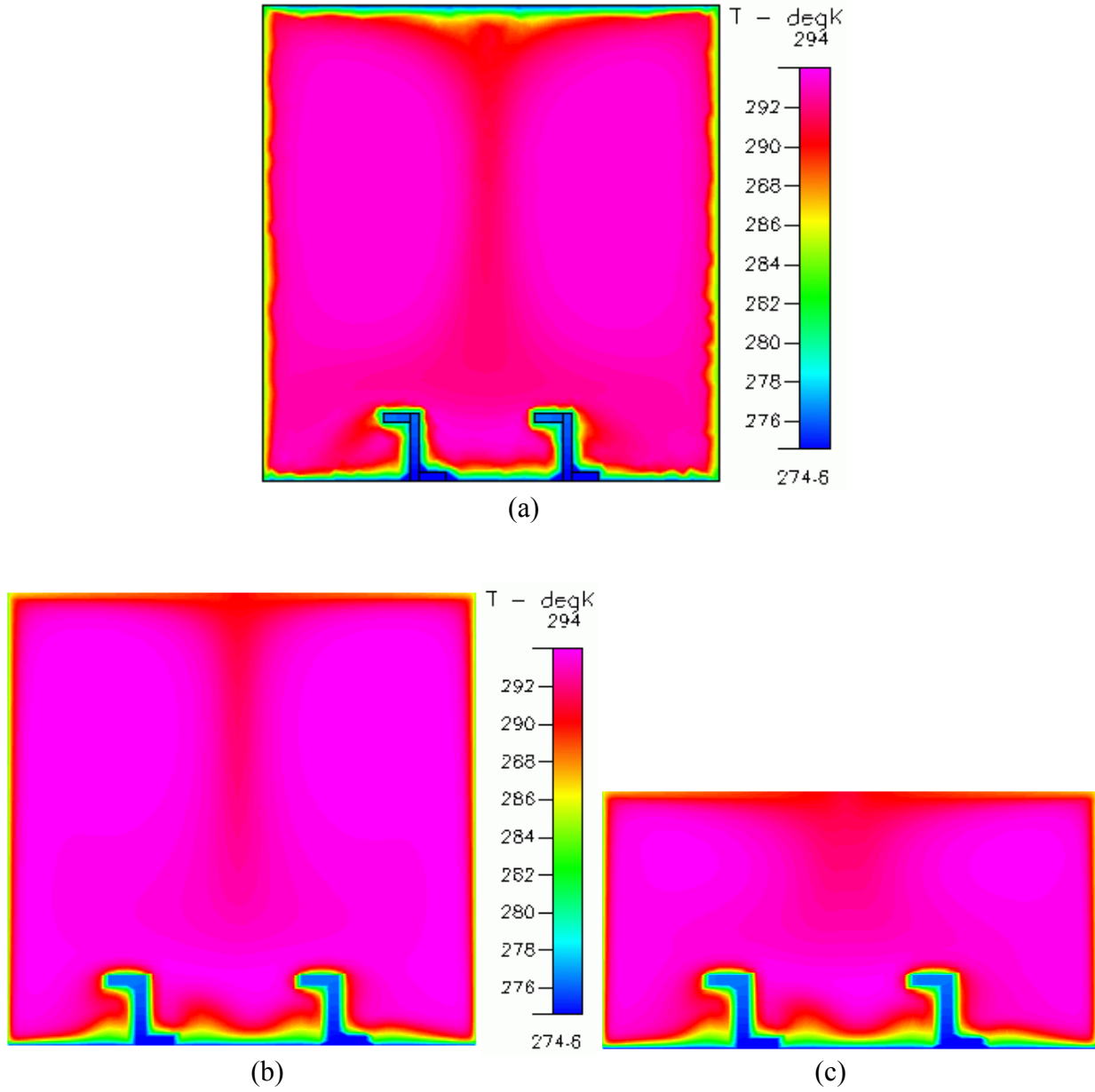


Figure 38. Temperature Contours for Two-Dimensional Simulations After 40 Minutes of Cooling for a (a) Full Tank or for Air Gap Heights of (b) 3.8 cm and (c) 26.5 cm

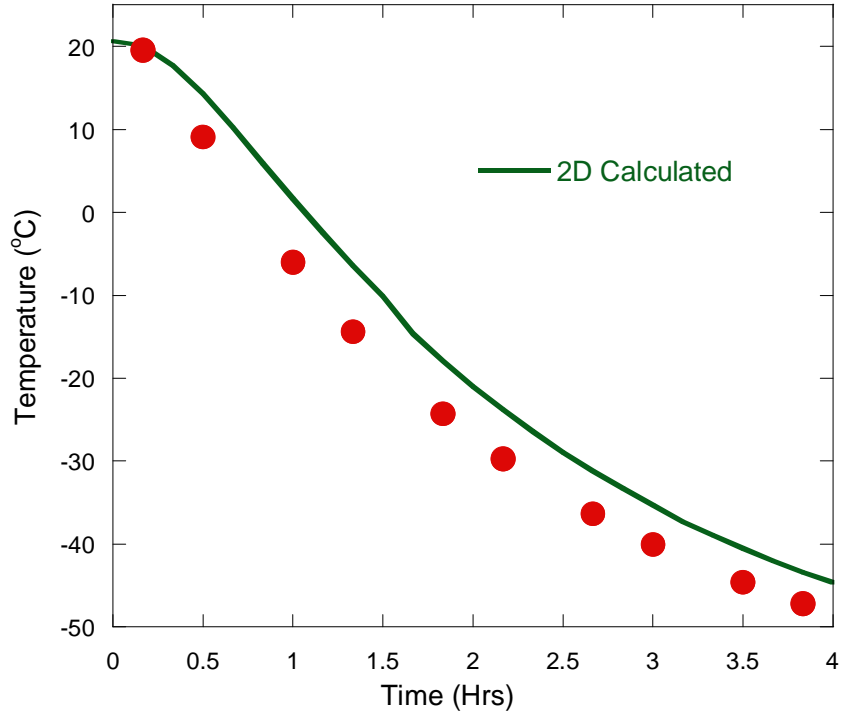


Figure 39. Measured and Calculated Temperatures From Two-Dimensional Simulations Near the Center of a Tank Compartment That Includes an Ullage Space (3.8 cm Height), With the Symbols Representing Measured Temperatures

#### 4.3.2 Three-Dimensional Simulations.

In many situations, the use of a two-dimensional numerical solution is limited, and a three-dimensional simulation is more appropriate. A variety of different three-dimensional simulations were performed for the wing tank simulator geometry. For the calculations, the three-dimensional unstructured grid shown in figure 40 was used. This tetrahedral grid is divided into 14 triangular unstructured domains comprised of 180,000 triangular cells including nearly 7,000 cells in the piccolo tube and 4,000 in each stringer. For the static flow simulations, the piccolo tube was omitted.

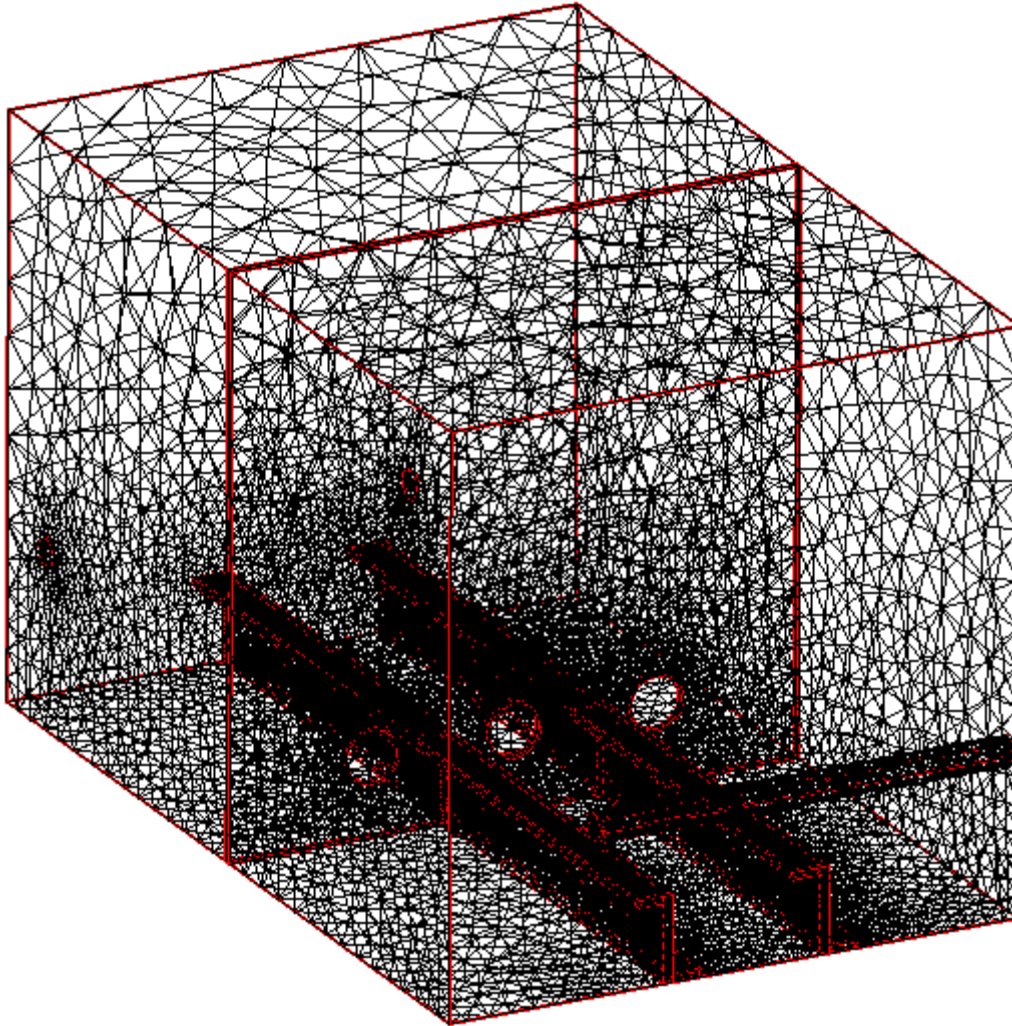


Figure 40. Three-Dimensional Unstructured Grid

Three-dimensional CFD calculations were used to study the temperature profile in the wing tank simulator during static cooling (Simulations 9 and 10, table 5). Figure 41 shows temperature contours for three- and two-dimensional simulations (two-dimensional plane near the center of the tank) after 4 hours. The boundary conditions are the same as the previous FAA simulations, and the skin temperatures follow the schedule of figure 30. The heat transfer with the center aluminum plate is significant, resulting in lower fuel temperature near the center in the three-dimensional simulation (figure 41(a)). As the wall effects were not considered, the profile from the two-dimensional calculation (figure 41(b)) does not represent the fuel temperature of all the locations in the tank. Moreover, figure 41(b) shows two large vortical cells, while figure 41(a) shows a more complex flow pattern, which changes with the location of the two-dimensional viewing plane in the tank. If the thermal plot of the three-dimensional simulation at a location near the center of a tank section is considered, the profile is similar to the two-dimensional result. Figure 42 compares both two- and three-dimensional, time-varying simulations of the temperature with measurements for the thermocouple located at 0.25 inch from the bottom, near the tank center. Figure 42 shows that for this location in the tank, the measured temperatures

agree much better with the three-dimensional simulations. The conduction, particularly from the baffle plate located at the center of the tank, was not taken into account in the two-dimensional calculations.

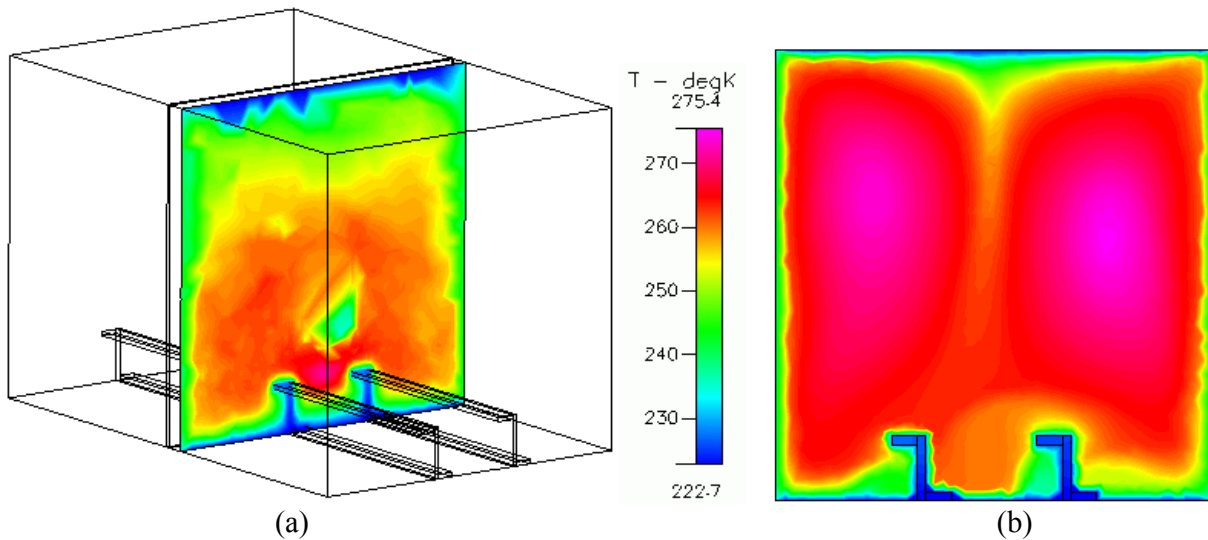


Figure 41. Comparison of Temperature Color Contour Plots Within the Wing Tank Simulator Simulated by (a) Three-Dimensional and (b) Two-Dimensional Calculations

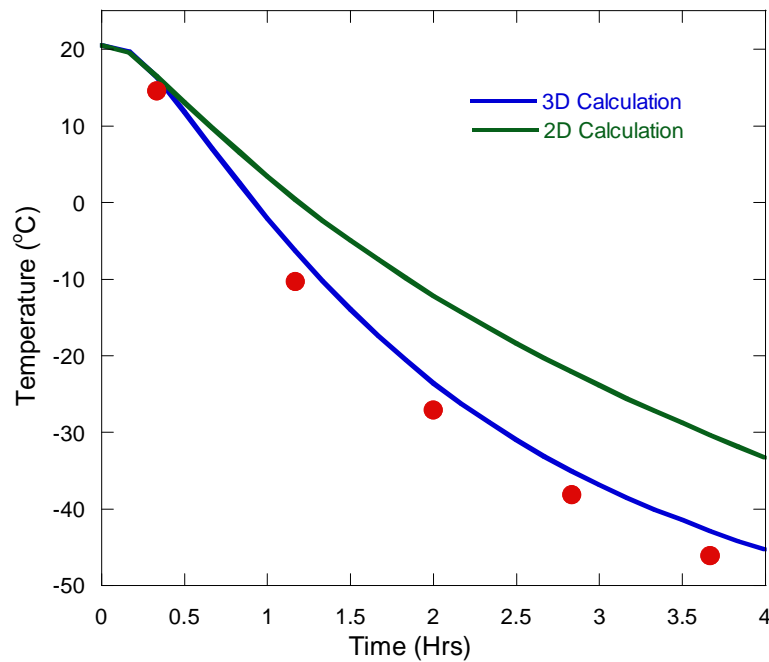


Figure 42. Temperature Measurements and Two- and Three-Dimensional Simulations at a Single Location for Different Times, With the Symbols Representing Measured Temperatures

A three-dimensional structured grid was used to determine how the temperature profile is affected when the wing tank simulator has an ullage space (Simulation 11, table 5). For the simulation, a 3.8-cm air gap height was considered. The horizontal and vertical walls were uniform in temperature and varied with time (Test 42, figure 30). In the three-dimensional simulations, the center plate in the tank played an important role, as it acts as an important heat conduction path, as do the stringers. Figure 43 shows that the three-dimensional calculations agree well with the temperature measurements (in contrast to the two-dimensional simulations shown earlier).

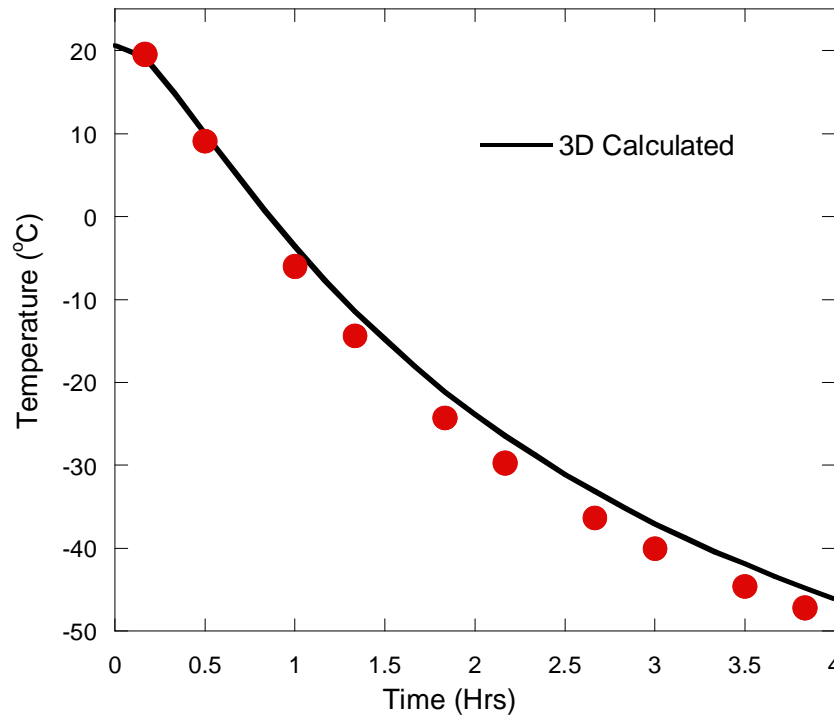


Figure 43. Measured and Simulated Temperatures for a Tank With an Ullage Space (3.8 cm Height), With the Symbols Representing Measured Temperatures

#### 4.4 MODELING SUMMARY.

CFD simulations were used to study the heat transfer in the Lockheed, Boeing, and present FAA experiments. A variety of steady-state and time-varying simulations were performed using structured grids, unstructured grids, and different tank geometries. It was found that relatively large variations (greater than 100%) in the viscosity of different fuel samples were required to produce significantly different temperature distribution within a fuel tank. More specifically, by analyzing two fuels with different viscosities, the results show that a viscosity difference of 10 to 15 cP did not change the temperature profile within the tank. In addition, relatively small differences (~5%) in the densities of the two fuels resulted in essentially the same heat transfer and flow for both fuels. Two-dimensional simulations can adequately represent the fluid dynamics within experimental fuel vessels at locations in which heat transfer effects in the third dimension are not significant (e.g., near the center of a tank compartment). However, often, a thermal boundary input in the third dimension cannot be neglected and three-dimensional

calculations are required. This is particularly true near the baffle rib, which separates the two compartments within the wing tank simulator. These calculations have shown that stringers, ribs, and other structural members within a fuel tank conduct heat from the fuel and strongly enhance fuel cooling. Their location and geometry should be considered in the thermal design of a fuel tank. Moreover, the results have shown that colder, denser fuel remains near the bottom surface of a tank near the stringers. Since this region near the stringers cools more rapidly than locations near the center of the fuel tank, a region near the stringers would be desirable for the location of thermocouples to indicate the coldest temperature in a fuel tank. In these studies of the effect of the ullage space on fuel tank heat transfer, it was found that an air gap insulates the upper surface of the liquid fuel and, thus, limits the heat transfer with the upper skin resulting in otherwise higher temperatures. From the perspective of limiting the cooling of jet fuel, an ullage space is desirable, and fuel tank designs that include stringers on the upper skin may not be preferred. The results indicate that CFD simulations provide important insights into the heat transfer and flow that occur in fuel tanks. Such information is important for understanding temperatures within wing tanks and may prove critical to the improved thermal design of future aircraft fuel tanks.

## 5. OTHER ISSUES.

### 5.1 IMPLICATIONS OF ADOPTING THE JET A-1 STANDARD.

One proposed solution to the danger of fuel freezing in aircraft fuel tanks was for the United States (U.S.) adoption of the Jet A-1 fuel standard. Jet A-1 fuel is the standard commercial jet fuel used outside the U.S. It has a freeze point specification temperature of  $-47^{\circ}\text{C}$  maximum (ASTM D 1655), which is  $7^{\circ}\text{C}$  below the Jet A specification. In 1995, the Defense Fuel Supply Center (DFSC) and the Air Transport Association (ATA) formed a task force to investigate the implications on fuel availability and the cost of converting CONUS (Continental United States) to Jet A-1. Members of the task force included representatives from DFSC, ATA, United States Air Force, Delta Airlines, Federal Express, US Air, Boeing Commercial Airplane Group, and Pratt & Whitney Aircraft. The potential benefits of this conversion were determined to be both logistical and operational. Logistically, conversion would have the benefit of creating a single, fungible jet fuel worldwide, which would reduce the costs of segregating and storing multiple fuel types. In addition, such a change could be beneficial for the military as a greater production of Jet A-1, with a  $-47^{\circ}\text{C}$  maximum freeze point, could increase the availability and lower the cost of JP-8 fuel, which also has a  $-47^{\circ}\text{C}$  maximum freeze point. The task force contacted numerous oil companies to determine the effect of this change on fuel cost and availability. Each of the major oil companies (e.g., Shell, Exxon, and Chevron) agreed that conversion to the Jet A-1 standard would reduce fuel availability from 10% to 15% in the U.S., with a corresponding increase in cost. The task force rapidly realized that the decreased availability and increased cost outweighed the perceived benefits of conversion.

Another less costly proposed solution is the targeted conversion of certain facilities to Jet A-1 fuel. Rather than converting the entire CONUS to Jet A-1, only certain airport facilities would be converted. These facilities and/or terminals would be those from which long-duration flights depart. Likely, this would include a handful of major airports, such as Chicago O'Hare International Airport, John F. Kennedy International Airport, and Los Angeles International Airport. This solution would have the benefit of providing lower freezing fuel only to the flights

that require it, while not decreasing the nationwide availability of jet fuel. In addition, fuel price increases averaged over all jet fuel purchased would likely be minimal. The major disadvantage of such a change would be logistical. The need for segregation and separate storage of Jet A-1 fuel at these airports would complicate fuel handling and possibly increase logistical costs.

## 5.2 FUEL SYSTEM HEATING.

Another solution to fuel freezing during a long-duration flight would be to use fuel heaters. Boeing has performed extensive investigations into potential options for using onboard heat sources for heating low-temperature fuel system components, such as wing tanks [19, 24, and 25]. In their analysis, two retrofit heat sources were selected as the most promising for the Boeing 747-200 aircraft: (1) an engine oil heat exchanger and (2) an electrical heating system. The engine oil heat exchange system offers a simple option, but it has relatively small and uncontrollable limitation on heat energy. The electrical heating system option is more complex and expensive, but it has better control and greater heating capability than the engine oil heat exchanger option. This work involved using Boeing's aircraft fuel tank thermal analyzer computer program for the prediction of fuel temperature based on variables such as initial fuel temperature, tank geometry and capacity, ambient route temperature, and flight route time. Analysis and experimental measurements show that fuel system heating is a viable technique to prevent fuel solidification. The disadvantages of fuel system heating are cost and the need to retrofit legacy aircraft.

Additional studies on the applicability of fuel system heating to current aircraft employed for long-duration flights are proposed.

## 6. CONCLUSIONS.

In the present work, the flowability and pumpability of jet fuel were studied to determine how changes in fuel properties at low temperature affect jet aircraft fuel system operation. Viscosity measurements as a function of temperature show that lower freeze point fuels tend to have higher viscosities near their freeze point than do higher freeze point fuels. These lower viscosities result in lower flow rates, as measured in a wing tank simulator. Thus, operation of aircraft fuel systems down to temperatures 3°C above the measured freeze point could result in lower flowability of the fuel than operation down to temperatures 3°C above the specification freeze point. The implications of these observations are likely dependent on the fuel system and aircraft being employed. In addition, computational fluid dynamics (CFD) methods were employed to create a model of the temperatures encountered in wing tank simulators. The calculations predict that completely full tanks, with a fuel-wetted upper surface, display relatively flat vertical temperature profiles, while fuel tanks with ullage space display significant fuel stratification, with colder fuel remaining near the bottom surface of the tank. These results show the importance of the location of fuel temperature sensors in obtaining accurate measurements of the lowest fuel temperatures in the tank. Future CFD work needs to explore more representative tank geometries, including tanks where one section has an ullage space and another section has a fuel-wetted upper surface to show the effect of heat transfer between these regions. Normal alkane analyses of the fuels studied show that the higher viscosity of lower freeze point fuels at their freeze point likely results from the fact that freeze point is a strong function of the larger normal alkanes present, while viscosity reflects the overall normal alkane fuel composition.

## 7. RECOMMENDATIONS.

The present work indicates that additional studies should be performed regarding operation of aircraft at fuel temperatures below the specification freeze point (but above the measured freeze point of the particular fuel sample). The viscometer results, which show that lower freeze point fuels tend to have higher viscosities than higher freeze point fuels near their freeze points, indicate that low freeze point fuels may not be as flowable or pumpable as higher freeze point fuels. The wing tank simulator results support and extend these observations, showing reduced flowability and pumpability of these lower freeze point fuels near their freeze points. The question is whether the reduced flowability is significant in the aircraft fuel systems of interest. This would probably need to be evaluated for each aircraft system experiencing long-duration polar routes. However, in some or all aircraft, fuel systems may have been designed conservatively enough that this reduction in fuel flowability may not be an issue.

The computational fluid dynamic results indicate that wing tanks may have severe fuel stratification, with colder fuel remaining near the bottom of the tank and not mixing with the bulk of the fuel. This indicates that fuel temperature sensors may not be properly indicating the coldest fuel temperatures. This issue is also likely dependent on the aircraft fuel system of interest, as the degree of stratification is a strong function of the presence of an ullage space in the particular fuel tank section, which is related to tank height and fuel level.

The results in studies of the freeze point of binary fuel mixtures indicate that the freeze point of fuel mixtures is a complex, nonideal function of the mixture fraction. Further experimental and computational studies need to be performed to determine the important factors that determine the freeze point of fuel mixtures.

## 8. REFERENCES.

1. Zabarnick, S. and Vangsness, M., "Properties of Jet Fuels at Low Temperature and the Effect of Additives," *Preprints-American Chemical Society, Division Petroleum Chemistry*, Vol. 47, 2002, pp. 243-246.
2. Turner, W.R., "Normal Alkanes," *Industrial and Engineering Chemistry, Product Research and Development*, Vol. 10, 1971, pp. 238-260.
3. Lewtas, K., Tack, R.D., Beiny, D.H.M., and Mullin, J.W., "Wax Crystallization in Diesel Fuel: Habit Modification and the Growth of n-Alkane Crystals," in *Advances in Industrial Crystallization*, Garside, J., Davey, R.J., and Jones, A.G., eds., Butterworth Heinemann, Oxford, 1991.
4. Stockemer, F.J., "Experimental Study of Low-Temperature Behavior of Aviation Turbine Fuels in a Wing Tank Model," NASA, CR-159615, 1979.
5. Coordinating Research Council, *Handbook of Aviation Fuel Properties*, 1983.
6. Zabarnick, S. and Widmor, N., "Studies of Jet Fuel Freezing by Differential Scanning Calorimetry," *Energy Fuels*, Vol. 15, 2001, pp. 1447-1453.

7. Coutinho, J.A.P., Mirante, F., Ribeiro, J.C., Sansot, J.M., and Daridon, J.L., "Cloud and Pour Points in Fuel Blends," *Fuel*, Vol. 81, 2002, pp. 963-967.
8. Claudy, P., Letoffe, J.M., Bonardi, B., Vassilakis, D., and Damin, B., "Interactions Between n-Alkanes and Cloud Point-Cold Filter Plugging Point Depressants in a Diesel Fuel. A Thermodynamic Study," *Fuel*, Vol. 72, pp. 821-7, 1993.
9. Zabarnick, S., Widmor, N., and Vangsness, M., "Studies of Urea Treatment on the Low-Temperature Properties of Jet Fuel," *Energy Fuels*, Vol. 16, 2002, pp. 1565-1570.
10. Coutinho, J.A.P., "A Thermodynamic Model for Predicting Wax Formation in Jet and Diesel Fuels," *Energy Fuels*, Vol. 14, 2000, pp. 625-631.
11. Chiu, G., "Technical Update: The Impact of Comingling Jet Fuel on Freezing Point," Phase Technology, 1993.
12. Chiu, G., "Test Report: Comingling Study of Jet Fuels," Phase Technology, 2000.
13. Atkins, P.W., *Physical Chemistry*, W.H. Freeman and Company, New York, 1986.
14. Widmor, N.M., Ervin, J.S., and Zabarnick, S., "Prediction of the Freeze Point Temperature of Jet Fuel Using a Thermodynamic Model," *Preprints-American Chemical Society, Division Petroleum Chemistry*, Vol. 47, 2002, pp. 239-242.
15. Coordinating Research Council, "Low Temperature Behavior of Fuels in Simulated Aircraft Tanks," CRC Report No. 532, 1983.
16. Desmarais, L.A. and Tolle, F.F., "Fuel Freeze Point Investigations," Aero Propulsion Laboratory, Wright-Patterson AFB, AFWAL-TR-84-2049, 1984.
17. McConnell, P.M. and Massmann, L.A., "Operational Effects of Increased Freeze Point Fuels in Thin Wing Aircraft," Aero Propulsion Laboratory, Wright-Patterson AFB, AFWAL-TR-82-2087, 1982.
18. McConnell, P.M., Massmann, L.A., Peterson, G.N., and Tolle, F.F., "Fuel/Engine/Airframe Trade-Off Study Operational Effects of Increased Freeze Point Fuels," Aero Propulsion Laboratory, Wright-Patterson AFB, AFWAL-TR-82-2067, 1982.
19. Mehta, H.K. and Armstrong, R.S., "Detailed Studies of Aviation Fuel Flowability," Boeing Commercial Aircraft Company, NASA CR-174938, 1985.
20. Friedman, R. and Stockemer, F.J., "Temperature and Flow Measurements on Near-Freezing Aviation Fuels in a Wing Tank Model," ASME, 80-GR-63, 1980.

21. Ervin, J.S., Zabarnick, S., Binns, E., Dieterle, G., Davis, D., and Obringer, C., "Investigation of the Use of JP-8+100 With Cold Flow Enhancer Additives as a Low-Cost Replacement for JPTS," *Energy Fuels*, Vol. 13, 1999, pp. 1246-1251.
22. Rider, W.J., Kothe, D.B., Mosso, S.J., Cerrutti, J.H., and Hochstein, J.I., "Accurate Solution Algorithms for Incompressible Multiphase Fluid Flows," AIAA, 95-0699, 1995.
23. Hirt, C.W. and Nichols, B.D., "Volume of Fluid (VOF) Method for the Dynamics of Free Boundaries," *Journal of Computational Physics*, Vol. 39, 1981, pp. 201-225.
24. Pasion, A.J., "Design and Evaluation of Aircraft Heat Source Systems for Use With High-Freezing Point Fuels," NASA, CR-159568, 1979.
25. Pasion, A.J. and Thomas, I., "Preliminary Analysis of Aircraft Fuel Systems for Use With Broadened Specification Jet Fuel," NASA, CR-135198, 1977.

APPENDIX A—FIGURES AND DRAWINGS OF THE BOEING 747 WING TANK AND FUEL SYSTEM

Figures courtesy of Kevin Longwell, Boeing.

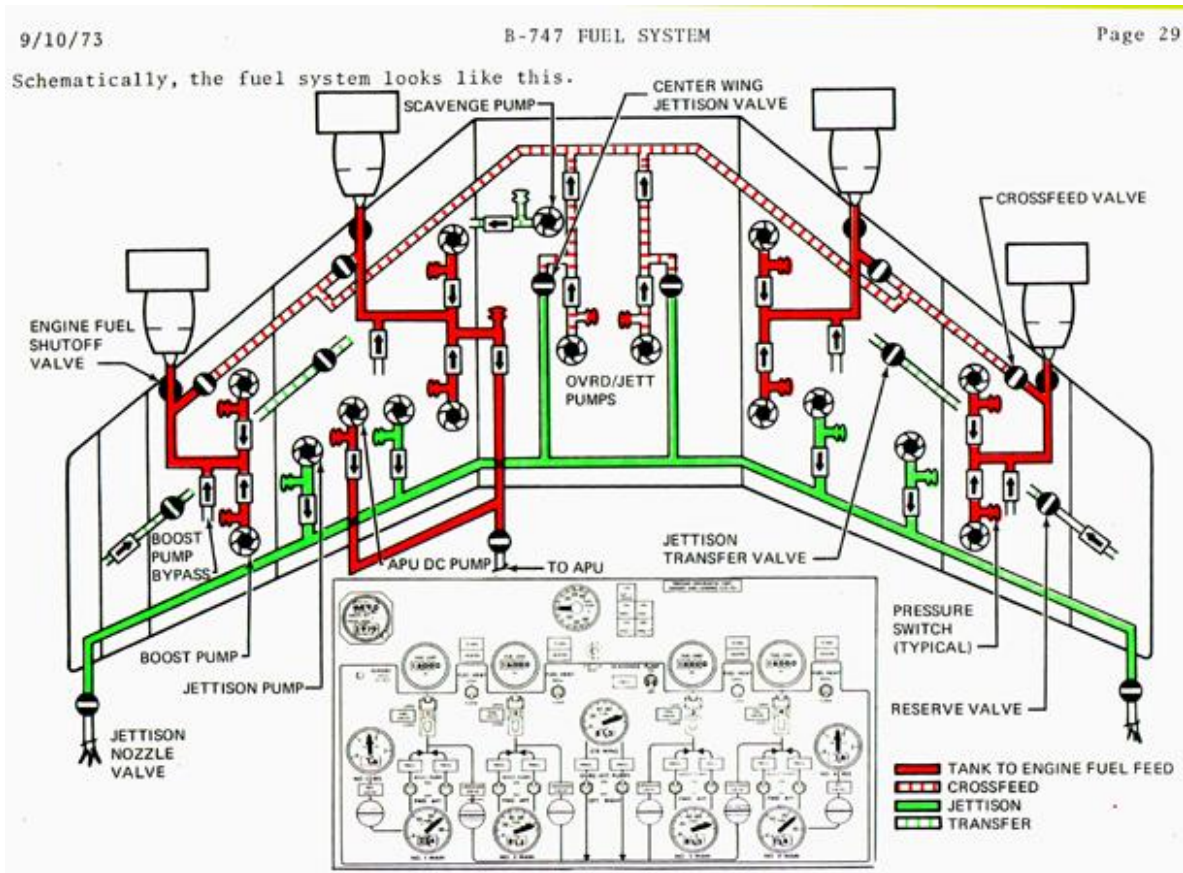


Figure A-1. Schematic of the Boeing 747 Fuel System

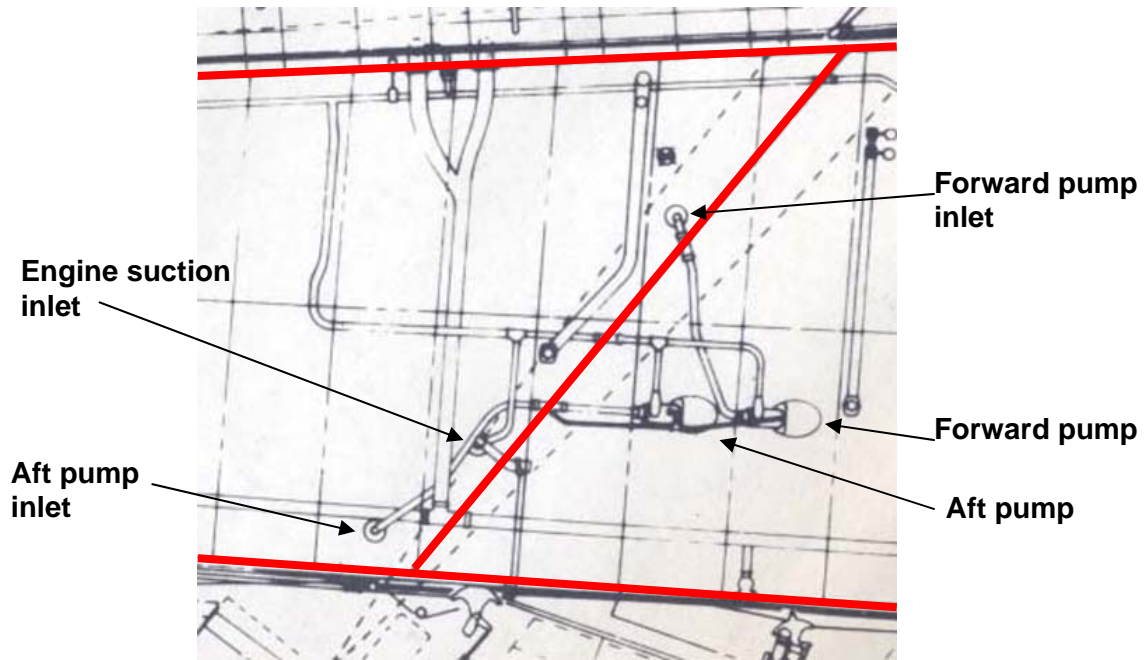


Figure A-2. Schematic of Boeing 747 Wing Showing Region Between Outboard Tank (No. 1 Main Tank, left of red line) and Inboard Tank (No. 2 Main Tank, right of red line) and Locations of the Forward and Aft Boost Pumps and Pump Inlets for the Outboard Tank



Figure A-3. Inboard Fuel Tank (No. 2 Main Tank) Showing Location of the Outboard Aft Boost Pump

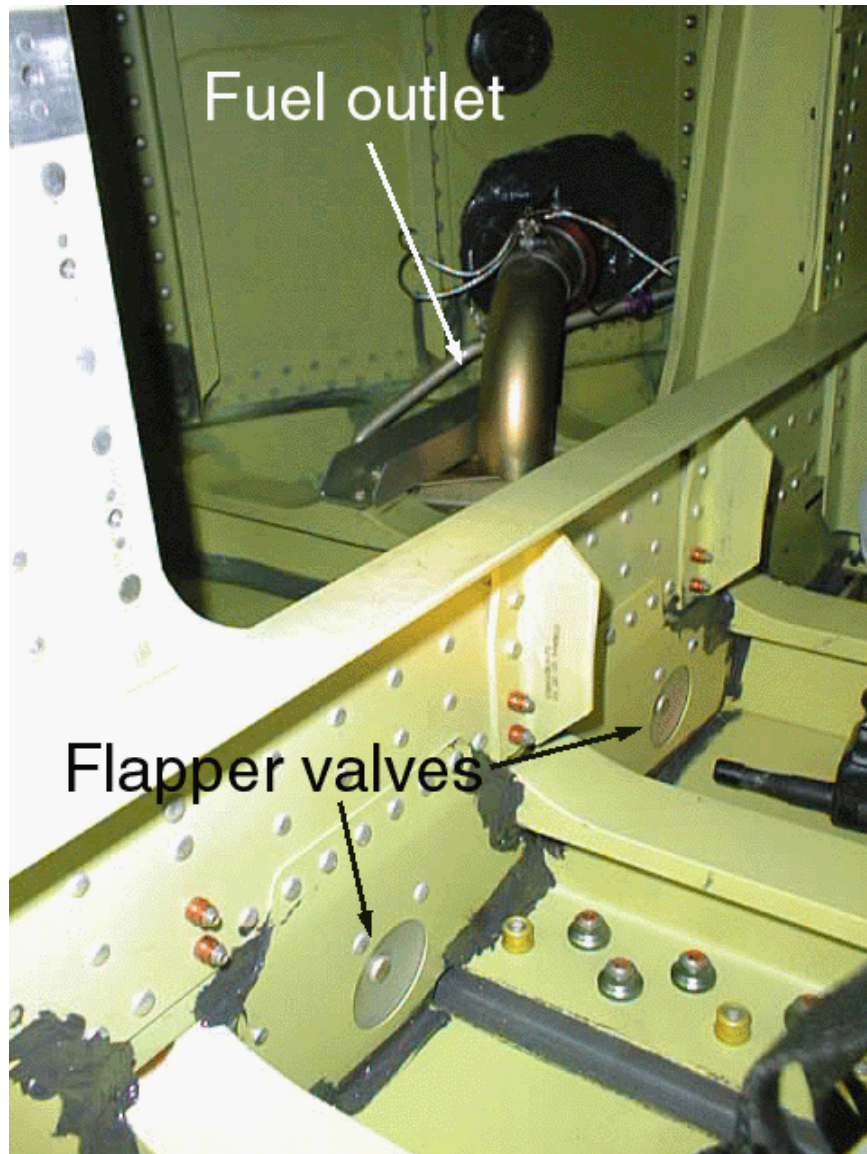


Figure A-4. Outboard Wing Tank (No. 1 Main Tank) Showing Location of Flapper Valves in Lower Baffle Rib and Forward Boost Fuel Inlet

APPENDIX B—PHOTOGRAPHS OF THE WING TANK SIMULATOR

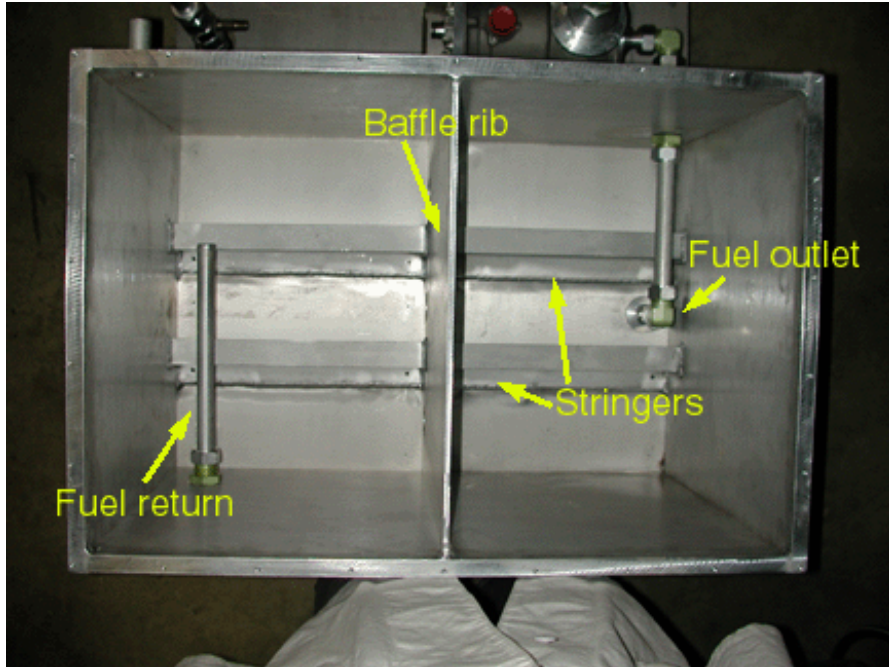


Figure B-1. Wing Tank Simulator Showing Location of Baffle Rib, Stringers, Pump Inlet, and Fuel Return Piccolo Tube



Figure B-2. Inside Wing Tank Simulator Showing Location of Flapper Valves

## APPENDIX C—BOOST PUMP INFORMATION

A Boeing 747 boost pump was acquired on loan from Hydro-Aire. The pump is Model No. 60-989100 Serial No. 019701753 contained within a housing unit Model No. 60B89004-5 Serial No. 07995488. The measured flow versus pressure pump curve for this pump is shown in figure C-1. The pump was powered with a Hobart AXA 2200 7.5 kVA Frequency Converter.

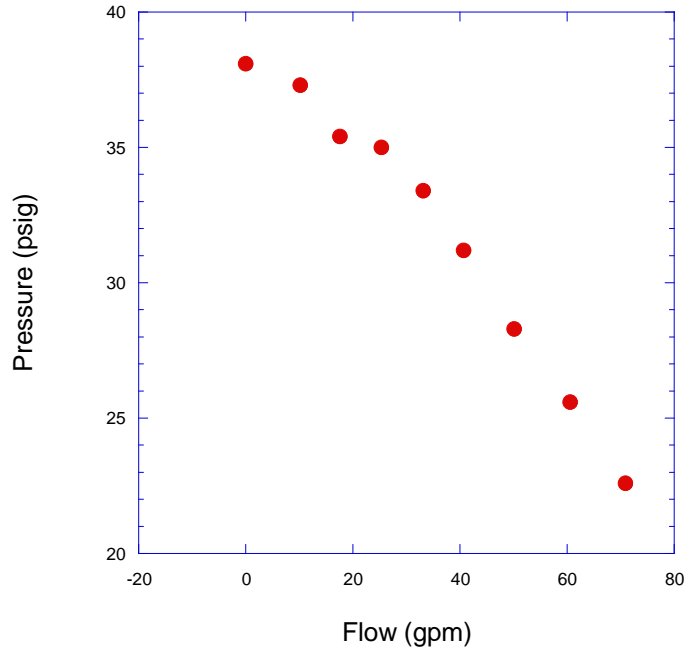


Figure C-1. Pump Curve for Boost Pump Showing Pressure vs Flow Rate

In addition, another boost pump was obtained from AirLiance Materials as a backup. This was a Model No. 60-75504 (Hydro-Aire) or 60B92404 (Boeing) boost pump Serial No. 11732604 with housing 60-75502 Serial No. 02721878.

APPENDIX D—WING TANK SIMULATOR RUNS PERFORMED

Table D-1. Wing Tank Simulator Runs Performed

Test Number	Date	Test type	Notes	Fuel
1	6/10/2002	Calibration and check out	Leak check out	3166
2	6/28/2002	Calibration and check out	Calibration of flow meter	3166
3	7/10/2002	Calibration and check out	Environmental chamber check out	3166
4	7/11/2002	Calibration and check out	Environmental chamber cooling capability	3166
5	7/15/2002	Calibration and check out	Circulating pump power test	3166
6	7/17/2002	Calibration and check out	Pump heating effects on the fuel and pump power changes with temperature	3166
7	7/19/2002	Calibration and check out	Pump heating effects on the fuel and pump power changes with temperature	3166
8	8/6/2002	Calibration and check out	Pump operation below freeze point of 3166 fuel	3166
9	8/7/2002	Calibration and check out	Circulating pump power supply monitored at temp below freeze point of 3166 fuel	3166
10	8/15/2002	Calibration and check out	Circulating pump flow rate at -48°C with 3166 fuel	3166
11	8/28/2002	Calibration and check out	Calibration of flow valve at 14°C	3166
12	9/10/2002	Recirculation and pump out	Comparing flow rates of circulated and pumped out of chamber 3166 fuel at -28°C	3166
13	9/11/2002	Recirculation and pump out	Comparing flow rates of circulated and pumped out of chamber 3166 fuel at -31°C	3166
14	9/12/2002	Recirculation and pump out	Comparing flow rates of circulated and pumped out of chamber 3166 fuel at -34°C	3166
15	9/20/2002	Recirculation and pump out	Comparing flow rates of circulated and pumped out of chamber 3166 fuel at -37°C	3166
16	9/24/2002	Recirculation and pump out	Comparing flow rates of circulated and pumped out of chamber 3166 fuel at -40.7°C	3166
17	9/26/2002	Recirculation and pump out	Comparing the flow rates of circulated and pumped out of chamber 3166 fuel at -42.5°C	3166
18	10/1/2002	Recirculation and pump out	Comparing the flow rates of circulated and pumped out of chamber 3166 fuel at +27°C. The circulating was stopped at -37°C.	3166
19	10/3/2002	Recirculation and pump out	Comparing the flow rates of circulated and out of chamber 3166 fuel at -45.1°C	3166
20	10/10/2002	Recirculation and pump out	Comparing the flow rates of circulated and pumped out of chamber 3166 fuel at -46.1°C. The circulating was stopped at -37°C.	3166

Table D-1. Wing Tank Simulator Runs Performed (Continued)

Test Number	Date	Test type	Notes	Fuel
21	10/17/2002	Recirculation and pump out	Comparing the flow rates of circulated and pumped out of chamber 4177 fuel at -56°C. The circulating was stopped at -37°C.	4177
22	12/2/2002		Changes to tank cooldown with insulation.	
23	1/15/2003	Recirculation and pump out	Comparing the flow rate of circulated and pumped out 4177 fuel at -55°C. The circulating was stopped at -37°C, and the pump motor power was monitored. Cooldown temps were recorded.	4177
24	2/6/2003	Recirculation and pump out	Comparing the flow rate of the circulated and pumped out 4177 fuel at -55°C. The circulation was stopped at -37°C, and the pump power was monitored. Cooldown temps were recorded.	4177
25	2/11/2003		Cooldown to -55°C using 4177 fuel.	4177
26	2/21/2003	Recirculation and pump out	Comparing the circulated and pumped out flow rates of 3166 at -45°C. The circulation was stopped at -37°C, and the pump power was monitored. Cooldown temps were recorded.	3166
27	3/5/2003	Recirculation and pump out	Comparing the circulated and pumped out flow rates of 3166 fuel at -47°C. The circulation was stopped at -37°C, and the pump power was monitored. Cooldown temps were recorded.	3166
28	3/19/2003	Recirculation and pump out	Comparing the circulated and pumped out flow rates of 4177 fuel at -57°C. The circulation was stopped at -37°C. The pump power was not monitored. The cooldown temps were recorded.	4177
29	3/28/2003	Recirculation and pump out	Comparing the circulated and pumped out flow rates of 2976 fuel at -62°C. The circulation was stopped -37°C. The pump power was monitored, and the cooldown temps were recorded.	2976
30	4/4/2003	Recirculation and pump out	Compare the circulated and pumped out flow rates of 2976 fuel at -62°C. The circulation was stopped at -37°C. Cooldown temps were recorded.	2976
31	4/23/2003	Recirculation and pump out	Compare the circulated and pumped out flow rates of 4177 fuel at -55°C. The circulation was stopped at -37°C. Two cooldowns were run; the second without insulation.	4177
After test 31 first cooldown the tank walls foam insulation was removed.				
32	5/21/2003	Recirculation and pump out	Compare the circulated and pumped out flow rates of 3804 fuel at -49°C. The circulation was stopped at -37°C at TC 11. Two cooldowns were run.	3804

Table D-1. Wing Tank Simulator Runs Performed (Continued)

Test Number	Date	Test type	Notes	Fuel
A new flow meter and pressure transducer for pump output pressure were installed after test 32 first cooldown.				
33	5/31/2003	Recirculation and pump out	Compare the circulated and pumped out flow rates of 3804 + 4314 (16000mg/L) at -60°C. The circulation was stopped at -37°C.	3804
34	6/3/2003	Recirculation and pump out	Compare the circulated and pumped out flow rates of 4177 fuel at -55°C. The circulation was stopped at -37°C. Cooldown temps were recorded.	4177
35	6/5/2003	Recirculation and pump out	Compare the circulated and pumped out flow rates of 3166 fuel at -47°C. The circulation was stopped at -37°C. Cooldown temps were recorded.	3166
36	6/9/2003	Recirculation and pump out	Compare the circulated and pumped out flow rates of 2976 fuel at -62°C. The circulation was stopped at -37°C. Cooldown temps were recorded.	2976
37	6/12/2003	Recirculation and pump out	Compare the circulated and pumped out flow rates of 3804 (16000 mg/L) fuel at -60°C. The circulation was stopped at -37°C. Cooldown was recorded.	3804
38	6/14/2003	Recirculation and pump out	Compare the circulated and pumped out flow rates of 4177 fuel at -55°C. The circulation was stopped at -37°C. Cooldown temps were recorded.	4177
39	6/17/2003	Recirculation and pump out	Compare the circulated and pumped out flow rates of 3804 fuel at -49°C. The circulation was stopped at -37°C. Cooldown was recorded.	3804
40	6/19/2003	Recirculation and pump out	Compare the circulated and pumped out flow rates of 3804 fuel at -49°C. The circulation was stopped at -37°C. Cooldown was recorded.	3804
A chiller plate was mounted on the bottom side of the tank and is insulated on the exposed side.				
41	7/10/2003	Recirculation and pump out	Compare the circulated and pumped out flow rates of 3804 fuel with a chiller plate attached to the tank bottom at -49° and -60°C chiller plate temp. The circulation was stopped at -37°C. Cooldown was recorded.	3804
42	7/16/2003	Recirculation and pump out	Compare the circulated and pumped out flow rates of 3804 fuel with a chiller plate attached to the tank bottom at -49° and -70°C chiller plate temp.	3804
43	7/24/2003	Recirculation and pump out	Compare the pump out and circulated flow rates of 3166 fuel with a chiller plate attached to the tank bottom. The chamber temp. was -47°C and the chiller temp. was -70°C.	3166
44	7/29/2003	Recirculation and pump out	Compare the pump out and circulated flow rates of 2976 fuel with a chiller plate mounted to the tank bottom. The chamber temp. was -62°C and the chiller temp. was -70°C.	2976

Table D-1. Wing Tank Simulator Runs Performed (Continued)

Test Number	Date	Test type	Notes	Fuel
A chiller plate was mounted on the bottom side of the tank and is insulated on the exposed side. (Continued)				
45	8/1/2003	Recirculation and pump out	Compare the pump out and circulated flow rates of 4177 fuel with a chiller plate mounted to the tank bottom. The chamber temp was -55°C and the chiller temperature was -70°C.	4177
A 1-inch inner diameter, 7-foot flex line was added to the pump out line.				
46	8/13/2003	Cooldown only	To examine the stratification of 4177 fuel with a chamber temp of -25°C and a chiller plate temp of -70°C.	4177
47	8/15/2003	Cooldown only	To examine the stratification of 4177 fuel with a chamber temp of -35°C and a chiller plate temp of -90°C.	4177
48	8/19/2003	Cooldown only	To examine the stratification of 3804 fuel with a chamber temp of -35°C and a chiller plate temp of -90°C.	3804
49	8/20/2003	Cooldown only	To examine the stratification of 3166 fuel with a chamber temp of -35°C and a chiller plate temp of -90°C.	3166
50	8/22/2003	Cooldown only	To examine the stratification of 2976 fuel with a chamber temp of -35°C and a chiller plate temp of -90°C.	2976
51	9/5/2003	Cooldown only	To examine the stratification of 2976 fuel with a chamber temp of -45°C and -55°C. The chiller plate temp. was set to -90°C.	2976
52	9/19/2003	Temperature flow limit	To determine the lowest pumpable temperature of the fuel	2976
53	10/3/2003	Temperature flow limit	To determine the lowest pumpable temperature of the fuel	3804
54	10/17/2003	Temperature flow limit	To determine the lowest pumpable temperature of the fuel	3166
55	11/7/2003	Temperature flow limit	To determine the lowest pumpable temperature of the fuel	4177
56	11/21/2003	Low flow	To evaluate the effect of relatively low flows (near 11 gpm) on low temperature flowability and pumpability	4177
57	12/3/2003	Low flow	To evaluate the effect of relatively low flows (near 11 gpm) on low temperature flowability and pumpability	3166
58	12/11/2003	Low flow	To evaluate the effect of relatively low flows (near 11 gpm) on low temperature flowability and pumpability	3804
59	1/14/2003	Low flow	To evaluate the effect of relatively low flows (near 11 gpm) on low temperature flowability and pumpability	2976